國立臺灣師範大學生命科學系碩士論文

中草藥抑制細胞興奮性毒殺以治療第十七型脊髓共濟失調症

Chinese herbal medicine as a new perspective for the treatment of spinocerebellar ataxia type 17 via inhibition of excitotoxicity

研 究 生：游賀培

He-Pei You

指導教授：吳忠信 博士

Chung-Hsin Wu. Ph.D.

林榮耀 博士

Jung-Yaw Lin. Ph.D.

中 華 民 國 103 年 2 月

目錄

中文摘要

在神經退化性疾病中過量麩胺酸誘導受器活化與神經細胞損傷具有關聯性，從過去文獻中發現在小腦脊髓萎縮症 (Spinocerebellar ataxia, SCA) 細胞模式中，當活化麩胺酸受器會使得胞外鈣離子大量流入細胞質中，影響粒線體致使其功能損傷，進而誘發細胞凋亡路徑，引發細胞死亡。其中 SCA17 其之發病機制為 TATA 結合蛋白 (TBP) 中多麩醯胺酸 (>42 glutamines) 擴增，無法有效與 DNA 結合，並與轉錄因子蛋白質結合導致轉錄活性受到抑制，細胞內蛋白質異常聚集，產生細胞壓力，最後引發細胞死亡；此外，亦發現鈣離子有大量流入細胞內的情況。本研究的目的篩選出對於神經退化性疾病具有改善作用之中草藥及其成分。實驗以 SH-SY5Y 神經母細胞瘤細胞為細胞模式，篩選各種中草材及其成分對於麩胺酸誘導細胞產生興奮性毒殺是否具有改善作用。以 MTT 和流式細胞儀分析方法，我們發現 NH043-1 有效降低麩胺酸誘導所造成的細胞死亡；從西方墨點法中，觀察 NH043-1 可以降低麩胺酸誘導六小時之後 Bax, Calpain-2 和 SBDPs 的表現量而 Bcl-2 的表現量有上升的趨勢；二十四小時之後 cleaved-PARP, cleaved-caspase-3 與 cleaved-caspase-9 的表現量有降低的趨勢。以 CL 冷光偵測儀，觀察 NH043-1 可以有效降低細胞內的自由基含量。利用流式細胞儀檢測粒線體膜電位，發現 NH043-1 可以提升粒線體膜電位。在誘導 nTBP/Q_{79}-EGFP 融合蛋白表現的 SCA17 細胞模式上，NH043-1 可以增加細胞的存活率以及 cleaved caspase-9, cleaved caspase-3 與

cleaved PARP 的表現量有降低的趨勢。在西方墨點法和 Dot-blot 方法，觀察 NH043-1 可以有效降低 TBP 蛋白質的異常聚集。在動物實驗部分使用 8 周大的 SCA17 轉殖基因老鼠從第九週開始注射 NH043-1，從 Rotarod assay 實驗發現在第 16, 18 及 20 周能夠有效延長其在 rotarod 上的時間，在 footprint assay 實驗上也改善步行缺失，並且在實驗小鼠小腦組織內有缺陷的 TBP 蛋白質的異常聚集和 cleaved-caspase-3 表現量都有減緩。據以上的結果，NH043-1 可以改善麩胺酸誘導所造成的細胞死亡，具有治療 SCA17 之潛力。

關鍵字：第十七型小腦萎縮症，以麩胺酸誘導之興奮性毒殺，SH-SY5Y 細胞，細胞凋亡。

Abstract

Excessive stimulation of glutamate induces neuronal damage through receptor-mediated excitotoxicity, which is thought to be involved in chronic neurodegenerative disorders**.** Several studies indicated that calcium influx into the cytoplasm in SCA transgenic cell by activation of glutamate receptors and increased toxic cascades, including the disturbance of mitochondrial function and the enhancement of apoptotic pathway. Spinocerebellar ataxia (SCA) type 17, a neurodegenerative disorder, is caused by polyglutamine (polyQ) expansion (>42 glutamines) in the basal transcription factor TATA binding protein (TBP). The polyQ expansion interferes, increases protein aggregation and results in cell death. It is believed that Chinese herbal medicines (CHMs) prescription might be a new perspective for the treatment of neurodegenerative disorder. Accordingly, we proposed to identify effective compounds of CHMs protecting cells from glutamate-induced excitotoxicity in human neuroblastoma SH-SY5Y cells. We found that NH043-1 protected human neuroblastoma SH-SY5Y cells from cell death induced by glutamate-mediated excitotoxicity, attenuated the production of intracellular reactive oxygen species (ROS), and decreased the expression of Calpain-2, SBDPs and Bax/Bcl-2 ratio for 6 h, and the expressions of cleaved-caspase-9, cleaved-caspase-3 and cleaved-PARP for 24 h. NH043-1 also blocked the decrease of mitochondrial membrane potential by MSG. In nTBP/Q_{79}-EGFP cell model, NH043-1 also showed the remarkably protective activity against the neuronal cell death and decreased the expression of cleaved-caspase-9, cleaved-caspase-3, and cleaved-PARP for 24 h. NH043-1 also inhibited the protein aggregation. In SCA17 animal model, NH043-1-treatment SCA17 mice performed better than Saline-treatment SCA17 mice on an accelerating rota-rod and

footprint experiments in 5 months. NH043-1 attenuated expression of TBP protein aggregation and cleaved-caspase-3 in cerebella of SCA17 mice. The results suggest that NH043-1 could be a potential medicine in the treatment of neurodegenerative disorders (SCA17) through inhibition of glutamate-induced apoptosis via mitochondria pathway.

KETWORDS: Spinocerebellar ataxia type 17, glutamate-induced excitotoxicity, SH-SY5Y cell, apoptosis.

Figure list

1 Introduction

1.1 Spinocerebellar Ataxias (SCAs)

SCAs are inherited in autosomal-dominant patterns, and the symptoms are lack of balance and exercise capacity resulted from dysfunctions of the cerebellum, signaling transductions, and signaling connections (Koeppen 2005, Carlson et al. 2009, Paulson 2009). During the past 15 years, there were approximately 35 various types of SCA identified according to distinct mutant genes. SCAs are categorized into three types depending on the genetic. The first, SCA1, 2, 3, 6, 7, and 17 are caused by the expansion of a CAG [encoding glutamine (Q)] repeat sequence located within the specific gene (Orr and Zoghbi 2007). The specific causing proteins could not fold correctly after translation, resulting in protein aggregates (Duenas et al. 2006, Orr 2012), which are believed to cause cell toxicity (Sakahira et al. 2002, Popiel et al. 2004). The second, SCA8, 10, and 12 are caused by the specific nitrogenous bases (CTG-, ATTCT-, and CAG-) repeat expansion of non-translation region resulting on particular genes (*KLHLIAS*, *ATXN10*, and *PPP2R2B*) variation (Margolis et al. 1993, Matsuura et al. 2000, Mutsuddi and Rebay 2005). The last, SCA5, 14, and 27 are aroused by

various mutations of specific genes (*SPTBN2*, *PRKCG*, and *FGF14*) including deletion, non-sense, translocation mutations (Chen et al. 2005, Misceo et al. 2009, Dick et al. 2012).

1.2 Spinocerebellar Ataxia 17 (SCA17)

SCA17 is a progressive and neurodegenerative disease, caused by a N-terminal aberrant polyQ expansion in TATA-binding protein (TBP), an essential transcription factor (Gostout et al. 1993, Koide et al. 1999, Nakamura et al. 2001). The range of the normal TBP polyQ tract is 25–42 Qs, which is encoded by a polymorphic mixed CAG/CAA trinucleotide repeat, whereas mutant TBP contains an expanded polyQ tract (>42 Qs) (Silveira et al. 2002, Reid et al. 2003, Rolfs et al. 2003). SCA17 is characterized by ataxia, progressive motor dysfunction, and degeneration of cerebellar Purkinje cells (Rolfs et al. 2003, Koeppen 2005, Kasumu and Bezprozvanny 2012). The underlying mechanisms remain unclear, but it has been shown that the calcium deregulation is involved in the pathogenesis of SCA17 transgenic mice (Duchen 2012). The mutant TBP protein in the mouse brain could result in the impairment of calcium homeostasis and excessive extracellular accumulation (Koeppen

2005, Ishikawa et al. 2009, Kasumu and Bezprozvanny 2012). In addition, mutant TBP-induced aggregation is associated with mitochondria dysfunction and caspase-dependent apoptosis (Lee et al. 2009, Matilla-Duenas et al. 2010). It has been suggested that the polyQ-expanded proteins are prone to aggregate to form nuclear or cytoplasmic inclusion that lead to neurodegeneration such as Huntingtin Disease or SCAs (Kim et al. 2002, Seidel et al. 2012). The presence of a polyQ stretch is critical for its recruitment into the aggregates (Uchihara et al. 2001). Several SCAs are associated with the presence of protein aggregates and apoptosis in a specific region of the brain (Ishikawa et al. 2009). In 2001, the CAG expansion in the TBP gene was discovered and subsequent studies found that expanded polyQ caused aggregation and intra-nuclear inclusion bodies (Nakamura et al. 2001, Friedman et al. 2009). Particularly, mutant TBP is also found in protein aggregates in other neurodegenerative disorders (Uchihara et al. 2001, Kim et al. 2002). In previous studies, the aggregation of polyQ-TBP was found to cause the release of cytochrome *C* from mitochondria into the cytoplasm and induced cell death in cellular model (Ghosh et al. 2007, Roshan et al. 2012).

1.3 Excitotoxicity

The over-activation of glutamate-related receptors: kainate acid (KA) receptor, N-methyl-d-aspartate (NMDA) receptor, α-amino-3-hydroxy-5-methylisoxazole-4-propionic acid (AMPA) receptor, and glutamatic metabotropic receptor, by extracellular accumulation of glutamate result in the open of receptor channels, leading to calcium imbalance (Mattson 2008, Lau and Tymianski 2010, Yang et al. 2011). A number of studies indicated that high concentration of glutamate is a potent neurotoxin capable of destroying neurons by apoptosis (Mattson 2008, Vaarmann et al. 2013). The reactive oxygen species (ROS) were subsequently increased by excessive calcium inflow, causing the dysfunction of mitochondria (Arundine and Tymianski 2004, Sun et al. 2010). Glutamatergic excitotoxicity is associated with the up-regulation of pro-apoptosis protein, Bax, and the down-regulation of anti-apoptosis protein, Bcl-2, that eventually induce the release of cytochrome *C* from mitochondria to cytoplasm (Liu and Zhu 1999, Dargusch et al. 2001, Chen et al. 2012, Ma et al. 2012). Previous study has indicated that neuronal apoptosis in response to stimulation of various glutamate receptors is mediated by caspase family

signaling (Hirashima et al. 1999, Delgado-Rubin de Celix et al. 2006, Di et al. 2010). In addition, the protein levels of both calpain-2 and calpain-specific alpha-spectrin breakdown products (SBDPs), which are both Ca^{2+}-dependent, were elevated in glutamate-induced cell injury (Anderton et al. 2011, Miao et al. 2012).

1.4 Oxidative stress

It is known that oxidative stress, induced by ROS or free radicals, plays an important role in the pathogenesis of neurodegenerative disorders (Li et al. 2013). The accumulation of calcium by mitochondria beyond the critical level perturbed functional activity and caused permeability transition in the inner mitochondrial membrane, leading to mitochondrial damage (Kristal and Dubinsky 1997) and neuronal death (Kroemer et al. 1998, McStay et al. 2002). It had been reported that increased mitochondrial calcium loading induced by glutamate is positively associated with ROS generation by mitochondria (Votyakova and Reynolds 2005). If mitochondria are affected or broken, the production of ROS is over-increased, resulting to oxidative stress and cell toxicity (Clausen et al. 2013).

Glutamatergic excitotoxicity has been shown to induce oxidative stress, which is associated with the dysfunction of mitochondria in neurodegenerative disorders (Lai et al. 2013). In addition, the decrease of cell viability and increased susceptibility to oxidative stress were observed in SCA3 cell model (Evert et al. 1999). The oxidative stress contributes to ATXN7 aggregation as well as toxicity, and anti-oxidants or inhibition of nitric oxide and nitrogen dioxide can ameliorate mutant ATXN7 toxicity (Ajayi et al. 2012).

1.5 Phytochemicals for the treatment of glutamate-induced cytotoxicity

Glutamate-induced apoptosis pathway is a potential target for developing neuroprotective agent, used for alleviating neurodegenerative diseases. In previous studies, asiatic acid, Ginsenoside Rd, Bis-(12)-hupyridone, and pinocembrin attenuated glutamate-induced cognitive deficits of mice and protected SH-SY5Y cells against glutamate-induced apoptosis *in vitro* (Gao et al. 2008, Xu et al. 2012, Zhang et al. 2012, Cui et al. 2013). Therefore, in this study, we studied Chinese herb medicine (CHMs) and their active compounds against

glutamate-induced excitotoxicity and SCA17 model.

2 Research aims

In this study, we screened the CHMs and their active compounds that could improve the symptoms of SCA17.

Three steps were set up:

(1) To study whether CHMs and the active phytochemicals inhibit the neurotoxicity mediated by glutamate by using the SH-SY5Y cell model

(2) To investigate the effects of active phytochemicals of CHMs on the cytotoxicity of nTBP/Q_{36}-EGFP and nTBP/Q_{79}-EGFP by using inducible SCA17 cell method

(3) To study that the phytochemicals improve defective phenotypes in the transgenic mice by SCA17 transgenic mice model

3 Materials and Methods

3.1 Materials

Human neuroblastoma SH-SY5Y cells were from ATCC. Dulbecco's Modified Eagle Medium with nutrient mixture F-12 (DMEM/F12), 0.5% Trypsin-EDTA, penicillin/streptomycin (P/S), and Fluo-4 AM were obtained from Invitrogen Corporation. Fetal bovine serum (FBS) was from Falcon.

Primary antibodies against Calpain-2, Bax, cleaved PARP, cleaved caspase-9, and cleaved caspase-3 were obtained from Cell Signaling Technology. Cytochrome C, Bcl-2, TBP (1C2) and TBP (N12) were purchased from Santa Cruz Technology. Actin and SBDPs was purchased from Millpore Corporation. Secondary antibodies of Horseradish peroxidase (HRP)-conjugated goat anti-mouse secondary antibody and goat anti-rabbit secondary antibody were obtained from Minipore Corporation.

3- (4,5-cimethylthiazol-2-yl)-2,5-diphenyl tetrazolium bromide (MTT) and retinoic acid (RA) was purchased from Sigma-Aldrich. Annexin V-FITC assay Kit was supplied from

BioVision Corporation. MitoProbe™ JC-1 Assay Kit was obtained from Invitrogen Corporation. Protease inhibitors cocktail were obtained from Roche Applied Science. Pure compounds were supplied by Sigma-Aldrich.

3.2 Cell culture

Human neuroblastoma SH-SY5Y cells, nTBP/Q_{36}-EGFP cells and nTBP/Q_{79}-EGFP cells, kindly supplied by Dr. Guey-Jen Lee-Chen, National Taiwan Normal University (NTNU), were cultured in DMEM/F12 supplemented with 10% FBS, 100 units/mL penicillin and 100 ug/mL streptomycin at 37 ºC in a 5% CO_2 humidified incubator, and cells were passaged until 80% to 90% confluency in a one tenth ratio.

3.3 MTT assay

This assay is based on the ability of succinate dehydrogenase to convert MTT into water-insoluble purple formazan crystals. Human SH-SY5Y neuroblastoma cells were plated in 96-well plates (2 x 10^4 cells/well). After 24 h, cells were pre-treated with the various concentrations of NH043-1 or

10 uM MK801 (NMDA receptor antagonist) for 1 h, and then challenged with 100 mM glutamate for 24 h.

To investigate the effects of NH043-1 on SCA17 inducible cell, nTBP/Q_{36}-EGFP and nTBP/Q_{79}-EGFP were seeded in 96-well plate (2 x 10^4 cells/well). After 24 h, cells were pre-treated with the various concentrations of NH043-1 for 1 d, and then challenged with 10 ug/mL doxycycline and retinoic acid (RA) for 1, 3, and 5 d.

After the treatment, 0.5 mg/ml MTT was added to culture media, and cells were incubated for 3 h at 37^{o}C. To dissolve the formazan crystals, 100 uL lysis solution [10% sodium dodecyl sulfate (SDS) and 0.01N HCl] was added and the absorbance was read at OD_{570} with an ELISA reader (uQuant, bio-tek INK, Vermont, USA). The blank control wells were used for zeroing absorbance. The percentage of cell viability was calculated as follows:

Cell viability (%) = (OD_{570} of experimental well / OD_{570} of control well) x 100%

3.4 Flow cytometric measurement of apoptotic cells

The apoptosis induced by glutamate was measured by flow cytometry by using Annexin V-FITC/propidium iodide (PI) double-labeling method. SH-SY5Y cells were seeded (1 x 10^6 cell/well) in 6 cm dish, and were treated with 100 mM glutamate and 15 uM NH043-1 or 10 uM MK801 for 24 h. Apoptotic cells were then trypsinized and collected by centrifugation at 2,000 rpm for 3 min. After washing with PBS, cells were then double-stained with Annexin V-FITC and PI. According to the manual, cells were resuspended in Annexin V-FITC binding buffer, incubated with Annexin V-FITC for 30 min, and were then incubated with PI. Samples were analyzed with a flow cytometery (FACS Sorter, Becton, Dickinson and Company) by two parameter-dot-plots, and a total of 10,000 cells were recorded in each case.

3.5 Western blotting

3.5.1 Preparation of cell lysates

Human SH-SY5Y neuroblastoma cells were treated with NH043-1 at indicated concentrations or 10 uM MK801 for 1 h, then challenged with 100 mM MSG. The nTBP/Q_{36}-EGFP and nTBP/Q_{79}-EGFP cells were treated with indicated concentrations of NH043-1, and then treated with 10 ug/mL doxycycline and RA for 5 d, washed with phosphate buffered saline (PBS), and then lysed with radioimmounoprecipitation buffer (RIPA) (150 mM NaCl, 50 mM Tris-HCl, 6 mM deoxycholate, and 1% Nonidet P-40 at pH 7.4) on ice for 5 min, followed by sonication and centrifugation at 13,000 rpm for 5 min at 4^{o}C.

3.5.2 Quantification of protein concentration

The protein concentrations were determined with bicinchoninic acid (BCA) protein assay kit (Thermo scientific). A standard curve was generated by serial dilution of bovine serum albumin (BSA) solutions, 800,

400, 200, 100, and 50 ug/mL in ddH_2O in a 96-well plate. One uL protein sample was mixed with 19 uL ddH_2O in well, and the BCA reagent was prepared by mixing 20 uL of solution A and 1 mL of solution B, then 100 uL of mixed solution was added to each well. The plate was incubated at 37°C for 30 min, and absorbance was read at OD_{562} with an ELISA reader.

3.5.3 Preparation of sodium dodecyl sulfate polyacrylamide gel electrophoresis (SDS-PAGE)

The separating solution was loaded to the glass sandwish, and 0.2% SDS was added slowly into the glass sandwish. After the separating gel became solid, upper liquid was removed, and the stacking solution was added into the glass sandwish. The gel was prepared after the gel was polymerized (Table 1).

Table 1. The formula of SDS-PAGE

	Separation gel			Stacking gel
Percentage	7.5%	10%	12.5%	
A solution	1.50 mL	2.00 mL	2.50 mL	0.45 mL
B solution	1.50 mL	1.50 mL	1.50 mL	
C solution				0.75 mL
ddH_2O	3.00 mL	2.50 mL	2.00 mL	1.80 mL
TEMED	9.0 uL			4.5 uL
10% APS	60.0 uL			13.0 uL

A solution: 30% acrylamide/bis-acrylamide.

B solution: 1.5M Tris-HCl and 0.4% SDS at pH 8.8.

C solution: 0.5M Tris-HCl and 0.4% SDS at pH 6.8.

TEMED: Tetramethylethylenediamine

APS: Ammonium persulfate.

3.5.4 Protein sample preparation

Protein samples were mixed with 4X protein loading dye (125 mM Tris-HCl, 4% SDS, 30% glycerol, and 0.2% bromophenol blue at pH 6.8), and heated at 95^{o}C for 5 minutes.

3.5.5 Electrophoresis

Equal amount of protein samples (40 mg) and the standard protein molecular weight marker were resolved on 7.5% or 12.5% SDS polyacrylamide gel electrophoresis. The electrophoresis apparatus was linked to an electric power provider with 70 V of the voltage and 20 mA of the current.

3.5.6 Semi-dry blotting

To perform semi-dry blotting, a polyvinylidene fluoride (PVDF) membrane and filter papers were cut and soaked with methanol, anode I buffer (0.3 M Tris-HCl and 10% methanol, pH 10.4), anode II buffer

(25 mM Tris-HCl and 10% methanol, pH 10.4), and cathode buffer (25 mM Tris-HCl, 40 mM glycine, and 10% methanol, pH 9.4). The transfer board was prepared on the experimental table, then one piece of paper with anode I buffer was plated on transfer board. Two pieces of paper with anode II buffer were placed on top of paper. The PVDF membrane was put on top of it, then, the gel was putted on the PVDF membrane, and three pieces of paper with cathode buffer were set on the top. The transfer apparatus was linked to electric power provider with 30 V of the voltage and 70 mA of the current for 80 min.

3.5.7 Immunoblotting

After semi-dry blotting, the PVDF membrane was stained with Ponceau S to verify the protein transferred to membrane. The PVDF was washed with TBST buffer (1M Tris-HCl, 5M NaCl, and 0.1% Tween-20, pH 7.4) to de-stain. The PVDF membrane was blocked with 5% non-fat milk solution in TBST at room temperature for 1 h or overnight at 4 ^{o}C. The PVDF

membrane was washed thrice with TBST for 5 min, then, incubated with primary antibody in dilute buffer (1% BSA, 0.05% Tween-20, and 0.02% NaN_3) at room temperature for 3 h or overnight at 4°C. After three quick washes in TBST buffer for 5 min, the membrane was treated with HRP-conjugated secondary antibodies for 1 h, and the proteins were visualized by using an enhanced chemiluminesence (ECL) detection reagent (Millipore) and detected with an ImageQuest™ LAS-4000 (Fujifilm Co., Tokyo, Japan). The expressions of protein were quantified by ImageJ (National Institute of Health, USA).

The percentage of neuroprotection was estimated as following: percentage of neuroprotection = 100%-[(X-Z)/(X-Y) x100%], X, the intensity of protein in control sample, Y, the intensity of protein in negative control, Z, the intensity of protein in CHMs-pretreated sample.

3.6 Measuring reactive oxygen species (ROS) activity in vitro by Chemiluminescence (CL)

The effects of NH043-1 on the ROS generations by glutamate-induced excitotoxicity in SH-SY5Y cells were measured by using CL analysis system**.** SH-SY5Y cells were plated in 6 cm dish (1 x 10^6 cells/dish) for 24 h, and the cells were pre-treated with 15 uM NH043-1 or 10 uM MK-801 for 1 h, then challenged with 100 mM MSG for 24 h. Then the cells were washed with PBS and lysed with 60 uL RIPA on ice for 5 min, and sonicated and centrifuged at 13,000 rpm for 20 min at 4^{o}C. The 200 uL protein samples (20 ug) were mixed with 0.5 mL of 0.2 mM luminal (5-amino-2, 3-dihydro-1, 4-phthalazinedione, Sigma). After 5 min, CL was measured by the amounts of chemiluminescence with a CL analysis system (CLD-110, Tohoku Electronic Inc. Co., Sendai, Japan).

3.7 Measuring mitochondrial membrane potential in vitro by flow cytometery

The effects of NH043-1 on the mitochondrial membrane potential by glutamate-induced excitotoxicity in SH-SY5Y cells

were measured by using flow cytometry with JC-1 dye staining**.** SH-SY5Y cells were plated in 6 cm dish (1 x 10^6 cells/dish) for 24 h, and then the cells were pre-treated with 15 uM NH043-1 or 10 uM MK-801 for 1 h, followed by being challenged with 100 mM MSG for 12 h. The cells were washed and collected by centrifugation at 2000 rpm for 3 min, and after washing with PBS, the cells were stained using JC-1 dye for 30 min. For positive control group, 5 uM carbonyl cyanide 3-chlorophenyl hydrazine (CCCP) was added to induce mitochondrial membrane depolarization. According to the kit's protocol, the cells were washed and re-suspended in PBS, and analyzed with a flow cytometer by two parameter dot-plots. A total of 10,000 cells were recorded in each case.

3.8 Dot-blot filter retardation assay

The effects of NH043-1 on the nTBP/Q_{36}-EGFP and nTBP/Q_{79}-EGFP aggregation in nTBP/Q_{36}-EGFP and nTBP/Q_{79}-EGFP SH-SY5Y cells, respectively, induced by doxycycline were measured by using BRL dot-blot instrument (Bio-Rad)**.** The nTBP/Q_{36} and nTBP/Q_{79} cells were plated in 6 cm dish (1 x 10^6 cells/dish) for 24 h, and the cells were

pre-treated with 15 uM NH043-1 for 1 h, then treated with 10 uM doxycycline and 10 uM RA for 5 d. The cells were washed and collected by centrifugation at 2,000 rpm for 3 min at 4 ^{o}C, and then removed PBS. The cells were incubated on ice for 30 min in the buffer (100 mM NaCl, 5 mM $MgCl_2$, 50 mM Tris-HCl pH 8.8, 0.5% NP-40, 100 mM EDTA, and cocktail). After centrifugation at 14,000 rpm for 5 min at 4 ^{o}C, the precipitates were dissolved with the buffer (15 mM MgCl2, 20 mM Tris-HCl pH 8.0, and 0.5 mg/mL DNase I) at 37 ^{o}C for 60 min. The protein concentrations were determined with bicinchoninic acid (BCA) protein assay kit (Thermo scientific). Twenty mg protein was mixed with 2% SDS solution to 0.2 mL and loaded to dot-blot machine through a cellulose acetate membrane. Membrane was washed with 0.1% SDS solution, blocked with 5% non-fat milk in TBST solution at room temperature for 1 h, and washed thrice with TBST for 5 min, then, incubated with primary TBP (N-12) antibody (1:1000) in dilute buffer overnight at 4^{o}C. After three quick washes in TBST buffer for 5 min, the membranes were treated with HRP-conjugated secondary anti-rabbit antibodies for 1 h, and the proteins were visualized by using an enhanced chemiluminesence (ECL) detection reagent (Millipore), and

detected with an ImageQuest^{TM} LAS-4000 (Fujifilm Co., Tokyo, Japan). The expressions of protein were quantified by ImageJ (National Institute of Health, USA)

3.9 Animal model

SCA17 transgenic mice bearing expanded TBP (Q_{109}) were kindly supplied by Dr. Hsiu-Mei Hsieh, NTNU. Mice were housed in individually ventilated cages with a 12 h light/dark cycle. All mice were bred and maintained in the animal facility at NTNU under specific pathogen-free conditions in accordance with institutional guidelines of The Animal Care and Use Committee at NTNU. The animals were used for motor behavioral assessments, footprint test, and western blotting analysis of aggregated TBP and cleaved-caspase-3 of the mouse cerebellum. The body weights of mice for rotarod test, and footprint test were measured twice a month.

3.9.1 Motor behavioral assessments

The mice were trained on the rotarod before drug treatment to establish the baseline of behavior activity

by using a linear acceleration from 2 rpm to 20 rpm over 5 min, and then maintained at 20 rpm for another 5 min. For experimental period, mice were placed with a linear acceleration from 4 to 30 rpm with over 5 min. The rotarod analysis was performed every two-week until 20th week. On every test, mice were subjected to three trials, each with a maximum duration of 600 sec and latency of fall was recorded. Mice were tested between 12:00 and 18:00.

3.9.2 Footprint patterns analysis

The test is widely used to determinate motor skill, coordination and balance. Hind- and forefeet of mice were coated with red and blue nontoxic paint, and the animals were allowed to walk along a runway over a fresh sheet of white paper. The distances between the center of the hind and preceding front footprint, length of steps and distance of parallel fore-paw/hind-paw were recorded over a sequence of six consecutive steps, excluding footprints made at the beginning and end of the run. The footprint patterns were determined

quantitatively by the measurements of stride length and fore-paw/hind-paw overlap. The tests were measured by every half of month.

3.9.3 Western blot analysis of aggregated TBP and cleaved-caspase-3 protein in the cerebellum of tested mice

All mice were anesthetized using urethane (1.5 mg/kg, *i.p*), and after 10 min, cerebella of mice (n=6, for each group) were collected in cold RIPA buffer, homogenized by 22G and 26G (32 mm and 13 mm) needles (TERUMO® Needle, NEOLUS) on ice, and stored at -80^{o}C. The protein concentrations of homogenates of cerebella were measured with bicinchoninic acid (BCA) protein assay kit (Thermo scientific). Then, 40 mg protein was resolved on 12.5% SDS-PAGE, and after electrophoresis and semi-dry blotting, the PVDF membrane was blocked with 5% non-fat milk solution in TBST at room temperature for 1 h or overnight at 4^{o}C. The PVDF was washed thrice with TBST for 5 min, then, incubated with primary

antibody in dilute buffer overnight at 4^{o}C. After three quick washes in TBST buffer for 5 min, the membrane was treated with HRP-conjugated secondary antibodies for 1 h, and the proteins were visualized by using an enhanced chemiluminesence (ECL) detection reagent (Millipore) and detected with an ImageQuest^{TM} LAS-4000 (Fujifilm Co., Tokyo, Japan). The expression of proteins was quantified by ImageJ (National Institute of Health, USA).

4 Results

4.1 NH043-1 effectively protects SH-SY5Y cells against MSG-induced excitotoxicity.

MTT assay, a colorimetric assay, was performed for measuring the activity of cellular enzymes representing the cell viability. MSG was used to induce excitotoxicity in neuroblastoma SH-SY5Y cell. First, cells were treated with 20, 40, 60, 80, and 100 mM MSG for 24 h to determine the $IC_{50\ toxicity}$ of MSG. The $IC_{50\ toxicity}$ of MSG was determined to be 100 mM for 24 h (Figure 1A), and 100 mM MSG was used with following experiments. Then, the IC_{50} of active compounds of CHMs on SH-SY5Y cells were measured, and half or one-fifth of compounds IC_{50} (1/2X or 1/5X IC_{50}) were used to screen the most effective compound against MSG. As shown in Table 1, NH043-1 exhibited 85% increased of cell viability, compared to MSG. Therefore, NH043-1 was chosen for further studies.

The treatment of SH-SY5Y cells with 5, 10, 15, 20, and 25 uM of NH043-1 against MSG for 24 h showed that 15 uM of NH043-1 significantly protected the cells against 100 mM MSG-induced excitotoxicity, exhibiting 85% cell viability, as 10

uM MK801 did. MK801 is an antagonist of NMDA receptor and was used as positive control in this study (Figure 1B). Collectively, our results indicate that NH043-1 showed a remarkably inhibitory effect on MSG-induced excitotoxicity.

4.2 NH043-1 attenuates the apoptosis of SH-SY5Y cells induced by MSG.

To examine whether NH043-1 inhibits apoptosis of SH-SY5Y cells mediated by MSG, flow cytometry analysis using Annexin-V staining, which is an apoptosis marker, was carried out. The results demonstrated that the treatment of 100 mM MSG for 24 h induced 54.13% apoptotic cells, however, NH043-1 at 15 uM and MK801 at 10 uM caused 9.04% and 9.73% apoptosis in the presence of MSG, respectively (Figure 2). It indicates that NH043-1 effectively reduced apoptosis of SH-SY5Y cells induced by MSG.

4.3 NH043-1 decreases the expressions of calpain-2 and SBDPs in SH-SY5Y cells treated with MSG.

To study whether NH043-1 protects SH-SY5Y cell apoptosis against MSG-induced excitotoxicity via calcium-dependent apoptosis, Western blot analysis was performed. Calpain-2, a thiol proteinase, is activated by the increases of intracellular free calcium ions and the reduction of Bcl-2 level, and SBDPs was elevated by calcium-induced calpain-2 in glutamate-induced cell death (Anderton et al. 2011, Miao et al. 2012). The calpain-2 and SBDPs were investigated. The 20% increments of both calpain-2 and SBDPs respectively were found by treating the cells with 100 mM MSG for 6 h. By pretreatment with 15 uM NH043-1 and MSG for 6 h, the expression of calpain-2 and SBDPs were decreased 200% and 250% (Figure 3). It indicates that NH043-1 significantly protected cell apoptotic death through calcium-induced apoptosis in MSG-treated SH-SY5Y cells.

4.4 NH043-1 decreases the expressions of Bax, but increases that of Bcl-2 in SH-SY5Y cells treated with MSG.

To study whether NH043-1 protects SH-SY5Y cell apoptosis against MSG-induced excitotoxicity via mitochondria-dependent apoptosis, Western blot analysis was performed. The increases of intracellular free calcium ions were related to the reduction of Bcl-2 level and the increment of Bax level (Anderton et al. 2011, Miao et al. 2012). The cell-survival protein, Bcl-2, and pro-apoptotic protein, Bax, which both mediate the release of cytochrome C from mitochondria, were investigated. The 50% increments of Bax, and the 40% decrement of Bcl-2, respectively were found by treating the cells with 100 mM MSG for 6 h. By pretreatment with 15 uM NH043-1 and MSG for 6 h, the expression of Bax were decreased 100%, while that of Bcl-2 was increased 150% (Figure 4). It indicates that NH043-1 significantly protected cell apoptotic death through mitochondria-dependent apoptosis in MSG-treated SH-SY5Y cells.

4.5 NH043-1 inhibits the expressions of caspase family proteins mediated by MSG.

Caspases, a family of cysteine proteases implicated in classical apoptotic death, were initially shown to play a role in delayed excitotoxic injury, which is associated with caspase-9, caspase-3 and nuclear enzyme PARP activation. To study whether NH043-1 protects SH-SY5Y cells death by MSG-induced excitotoxicity through caspase-dependent apoptosis, Western blot analysis was carried out. Treating the cells with 100 mM MSG for 24 h resulted in the 40%, 60%, and 190% increases of cleaved-caspase-9, cleaved-caspase-3, and cleaved-PARP respectively. By treating 15 uM NH043-1 against MSG for 24 h, the expressions of cleaved-caspase-9, cleaved-caspase-3, and cleaved-PARP, were significantly decreased 125%, 87%, and 52% inhibition, respectively, that of MSG treated cells, suggesting that NH043-1 increased cell viability by inhibiting the expressions of caspase family proteins in MSG-treated SH-SY5Y cells (Figure 5).

4.6 NH043-1 inhibits the intracellular ROS induced by MSG.

The glutamate-induced cytotoxicity was associated with mitochondrial dysfunction and increased ROS production in neuronal cells (Votyakova and Reynolds 2005). To investigate that NH043-1 would inhibit the accumulation of ROS implicated by MSG-induced excitotoxicity, the ROS level was measured by CL assay. Luminol is activated with an oxidant to exhibit its chemiluminescence. The emission spectrum is blue glow and can be detected with a chemiluminescence detector. We found that the intracellular ROS was 80% increment by 100 mM MSG-induced excitoxtoicity, but extracellular ROS was not affected. By treating with 10 uM NH043-1 or 10 uM MK801 for 24 h after MSG treatment, the intracellular ROS was 80% inhibition and the extracellular ROS did not alter (Figure 6). The results suggested that NH043-1 reduced the intracellular ROS production induced by MSG.

4.7 NH043-1 blocks the decrease of mitochondrial membrane potential (MMP) mediated by MSG.

To study whether NH043-1 blocks the decrease of MMP in SH-SY5Y cells mediated by MSG, flow cytometry analysis was performed. JC-1 dye could be used as an indicator of mitochondrial membrane potential in a variety of cell types. The results demonstrated that the treatment of 100 mM MSG exhibited 62±10% MMP in relative to that of the control after 24 h MSG treatment. However, NH043-1 at 15 uM showed 85±13% MMP by MSG and the treatment of 10 uM MK801 showed 90±5% MMP. Five uM CCCP, the disruptor of electron transport chain, showed 18±10% MMP (Figure 7). It suggested that NH043-1 effectively reduced the loss of MMP in SH-SY5Y cells arose by MSG.

4.8 NH043-1 effectively increases cell viability against Dox-induced nTBP/Q_{79}-EGFP cells.

To further study the effect of NH043-1 on SCA17, inducible nTBP/Q_{36}-EGFP and nTBP/Q_{79}-EGFP cells were used. The cells were induced with 10 ug/mL Dox to express

nTBP/Q_{36}-EGFP and nTBP/Q_{79}-EGFP with or without 15 uM of NH043-1 for 5 d. The cell viability was not changed at each group in nTBP/Q_{36}-EGFP. The treatment of 15 uM NH043-1 protected the cells against nTBP/Q_{79}-EGFP-induced cytotoxicity for 5 d, and the increase of 20% cell viability was observed. It indicates that NH043-1 showed a protective inhibitory effect on nTBP/Q_{79}-EGFP-induced cytotoxicity (Figure 8A).

4.9 NH043-1 inhibits the expression of caspase family proteins mediated by Dox-induced nTBP/Q_{79}-EGFP cells.

To study whether NH043-1 protects cell death induced by nTBP/Q_{79}-EGFP expression through caspase-dependent apoptosis, Western blot analysis was carried out. The 190%, 80%, and 90% up-regulation of cleaved-caspase-9, cleaved-caspase-3, and cleaved-PARP, respectively, were observed after inducing nTBP/Q_{79}-EGFP expression with 10 uM Dox for 5 d. The treatment of 15 uM NH043-1 significantly decreased the expressions of cleaved-caspase-9, cleaved-caspase-3, and cleaved-PARP, resulting in 88%, 100%, and 44% inhibition, respectively (Figure 8B and 8C). It suggests

that NH043-1 increased cell viability by inhibiting the expressions of caspase family proteins induced by nTBP/Q_{79}-EGFP expression through caspase-dependent apoptosis.

4.10 Effects of NH043-1 on polyQ protein aggregation by Dox-induced nTBP/Q_{36}-EGFP and nTBP/Q_{79}-EGFP cells.

To investigate whether NH043-1 decreases protein aggregation by Dox-induced in nTBP/Q_{79}-EGFP SH-SY5Y cells, dot-blot assay and Western blot were performed. nTBP/Q_{79}-EGFP protein aggregates were increased higher than that of nTBP/Q_{36}-EGFP by dot-blot and western blot analysis, after inducing with 10 uM Dox for 5 d. However, 15 uM NH043-1 significantly decreased the amounts of nTBP/Q_{79}-EGFP protein aggregates, 67% and 90% inhibition examined by dot-blot and Western blot analysis, respectively (Figure 9). It suggests that NH043-1 increased cell viability by inhibiting the protein aggregation of nTBP/Q_{79}-EGFP proteins.

4.11 NH043-1 ameliorates the neurological behavior of SCA17 transgenic mice.

To investigate the therapeutic effect of NH043-1 for SCA17 *in vivo*, a SCA17 transgenic mouse model was used (Ref). From 10- to 20-week-old mice, the body weights of SCA17 transgenic mice were not much different from those of control mice (Figure 10A). The experiments were carried out by *i.p*. administration of 4.5mg/kg of NH043-1 in saline to SCA17 transgenic mice once every two days from 8-week to 20-week, whereas control mice were given saline. First, motor coordination was examined by rotarod performance, and the results showed that saline-treated SCA17 mice, 269±36 seconds in the average of falling time was shorten than that of control mice group, 558±33 seconds, but it was improved in NH043-1-treated SCA17 mice, 393±36 seconds comparing with that of saline-treated SCA17 mice at 20 weeks (Figure 10B). Furthermore, the footprint patterns were measured to estimate left and right paw overlaps. We found that left and right paw overlaps of saline-treated SCA17 mice were 1.5±0.2 cm and 1.6±0.2 cm, respectively, longer than that of WT mice, 0.6±0.1 cm for left paw and right paw. However, the paw overlaps of SCA17 mice were shorter in NH043-1-treated

SCA17 mice to 0.8±0.1 cm and 1.1±0.1 cm for left and right paw, respectively, comparing with that of the saline-treated SCA17 mice (Figure 11). The results indicated that NH043-1-treated rescued the motor coordination deficits in SCA17 mice.

4.12 NH043-1 attenuates TBP/polyQ aggregation and cleaved-casapase-3 protein in cerebella of SCA17 mice.

To examine whether the NH043-1 treatment decreases the TBP/polyQ proteins aggregation and cleaved-caspase-3 proteins expression in SCA17 mice cerebella, we measured TBP/polyQ proteins aggregation and the level of cleaved-caspase-3 protein in cerebella of mice brain, and the results indicates that the up-regulation of aggregated TBP/polyQ proteins and cleaved-caspase-3, was both 100% in the cerebella of 20-week saline-treated SCA17 mice, comparing with that of control mice. Interestingly, 4.5mg/kg NH043-1-treated SCA17 mice showed the decrease of the expressions of aggregated TBP/polyQ and cleaved-caspase-3, 100% and 25%, respectively, indicating that NH043-1 significantly inhibited the expression of aggregated

TBP/polyQ and cleaved-caspase-3 in cerebella of SCA17 mice (Figure 12).

5 Discussion

Recently, CHMs have been used for the treatment of neurodegenerative disorders through the alterations in different receptor-mediated pathways, such as oxymatrine showing partial protection in the cortical neurons via down-regulation of NR2B containing NMDA receptors and up-regulation of Bcl-2 family (Zhang et al. 2013). Glutamate is the predominant excitatory neurotransmitter in the CNS, and excessive cellular glutamate release has been connected to excitotoxic events in neurodegenerative disease, where excessive glutamate binding to specific receptor, such as NMDA receptor, results in cell death (Mattson 2008, Lau and Tymianski 2010, Yang et al. 2011). In the present study, we observed MSG-mediated excitotoxicity in a dose-dependent manner in SH-SY5Y cells (Figure 1A), and screened many kinds of compounds from CHMs against MSG. NH043-1 was found to increase cell viability of MSG-induced in SH-SY5Y cells (Figure 1B). In addition, NH043-1 pretreatment protected the cells from apoptosis induced by MSG in SH-SY5Y cells, demonstrated by Annexin-V/PI staining followed by analysis with flow cytometry (Figure 2). Conclusively, NH043-1 exhibits protective effects on MSG-induced excitotoxicity

Exploration of mechanism underlying implies that glutamate excitotoxicity is related to the loss of mitochondrial membrane potential and calcium imbalance (Abramov and Duchen 2008, Pivovarova et al. 2013). The increase of cytosolic calcium in glutamate-treated hippocampal neurons triggered calpain activation (Brustovetsky et al. 2010). Besides, glutamate-mediated excitotoxicity induced apoptosis through mitochondrial apoptotic pathway (Pfeiffer et al. 2013, Zhang et al. 2014). The mitochondrial pathway plays an important role in neurodegenerative disorders. Cytochrome *C* releasing from the inter-membrane of mitochondria into cytoplasm binds Apaf-1, leading to the activation of caspase-9 and caspase-3. In addition, mitochondrial apoptotic pathway is mediated by members of the Bcl-2 family, such as Bax and Bcl-2 (Rana et al. 2007), that may have particularly important roles in mediating or protecting against calcium-mediated neuronal death by modifying mitochondrial membrane permeability (Chen et al. 2012, Duchen 2012). In this study, several pieces of evidence demonstrated that NH043-1 inhibited SH-SY5Y cells apoptosis by MSG through mitochondrial pathway. NH043-1 inhibited the MSG-induced calcium-dependent protein, calpain-2, SDBPs, and pro-apoptotic protein, Bax, but increased anti-apoptotic protein, Bcl-2 in SH-SY5Y cells (Figure 3 and Figure 4), as well as decreased the

cleaved-caspase-9, cleaved-caspase-3, and cleaved-PARP in SH-SY5Y cells (Figure 5), suggesting that NH043-1 could prevent mitochondria-mediated apoptosis.

Over-loading of calcium in neuron cells initiates the loss of mitochondrial membrane potential and produces ROS, leading to apoptosis (Lin and Beal 2006, Duchen 2012, Pfeiffer et al. 2013). In this study, we observed that NH043-1 inhibited the loss of mitochondrial membrane potential and the production of ROS (Figure 6 and Figure 7).

The neuroprotective effects of NH043-1 on AD were explored in recent years, and NH043-1 was first showed to prevent memory impairment and oxidative damage induced by $A\beta_{25-35,}$ suggesting that NH043-1 may be a potential therapeutic agent against AD Furthermore, NH043-1 was also demonstrated to inhibit Aβ aggregation. In addition to AD model, the applications of NH043-1 on other neurodegenerative diseases are rarely defined. This study was designed to investigate the effect of NH043-1 on SCA17 cells and transgenic mice model. We demonstrated that NH043-1 increased cell viability and decreased the expression of cleaved-caspase-9,

cleaved-caspase-3, and cleaved-PARP in nTBP/Q_{79}-EGFP SCA17 cells (Figure 8).

Protein misfolding and aggregation in the brain have been implicated as a common molecular pathogenesis of various neurodegenerative diseases (Proctor et al. 2010, Chang et al. 2011, Burke et al. 2013). SCA17 is characterized by protein aggregates in N-terminal region of TBP and selective loss of cerebellar neurons, particularly Purkinje cells (Koide et al. 1999, Nakamura et al. 2001, Orr and Zoghbi 2007). Therefore, SCA17 could share a common molecular mechanism leading to neuronal cell death mediated by protein aggregation (Chang et al. 2011, Huang et al. 2011, Roshan et al. 2012). We demonstrated that NH043-1 effectively suppressed aggregate formation by using Western blot and dot-blotting assay in nTBP/Q_{79}-EGFP SCA17 cells (Figure 9).

The pathogenesis of the SCA17 transgenic mice recapitulates the aggregation of protein, the loss of Purkinji cells, the motor coordination deficits, and cerebellum atrophy observed in SCA17 patients (Friedman et al. 2008, Chang et al. 2011). We demonstrated that NH043-1 improved the motor performance on an accelerating rotarod (Figure 10B) and ameliorated gait abnormalities, including

shortening the front/hind footprint overlaps and increasing the front/hind stride and parallel length (Figure 11). The analysis of TBP aggregation and cleaved-caspase-3 in 6-month-old SCA17 transgenic mice showed that NH043-1 decreased the formation of TBP aggregates and the expression of cleaved-caspase-3 in the cerebella of SCA17 mice (Figure 12). According to the above-mentioned results, NH043-1 improved the pathogenesis of SCA17 through inhibiting mitochondrial-mediated apoptotic pathway and decreasing TBP aggregation.

Present investigation revealed significantly that NH043-1 had protective effects on MSG-induced apoptosis of SH-SY5Y cells and nTBP/Q_{79}-EGFP SCA17 cells, and improved motor behavior of SCA17 transgenic mice. Taken together, we demonstrated the neuroprotective effects of NH043-1, which could be considered as a potential therapeutic drug for the treatment of SCA17 disease.

6 References

1. Abramov AY, Duchen MR (2008) Mechanisms underlying the loss of mitochondrial membrane potential in glutamate excitotoxicity. Biochimica et biophysica acta 1777:953-964.
2. Ajayi A, Yu X, Lindberg S, Langel U, Strom AL (2012) Expanded ataxin-7 cause toxicity by inducing ROS production from NADPH oxidase complexes in a stable inducible Spinocerebellar ataxia type 7 (SCA7) model. BMC neuroscience 13:86-92.
3. Anderton RS, Meloni BP, Mastaglia FL, Greene WK, Boulos S (2011) Survival of motor neuron protein over-expression prevents calpain-mediated cleavage and activation of procaspase-3 in differentiated human SH-SY5Y cells. Neuroscience 181:226-233.
4. Arundine M, Tymianski M (2004) Molecular mechanisms of glutamate-dependent neurodegeneration in ischemia and traumatic brain injury. Cellular and molecular life sciences: CMLS 61:657-668.
5. Brustovetsky T, Bolshakov A, Brustovetsky N (2010) Calpain activation and Na^+/Ca^{2+} exchanger degradation occur downstream of calcium deregulation in hippocampal neurons exposed to excitotoxic glutamate. Journal of neuroscience research 88:1317-1328.
6. Burke KA, Yates EA, Legleiter J (2013) Biophysical insights into how surfaces, including lipid membranes, modulate protein

aggregation related to neurodegeneration. Frontiers in neurology 4:17.

7. Carlson KM, Andresen JM, Orr HT (2009) Emerging pathogenic pathways in the spinocerebellar ataxias. Current opinion in genetics & development 19:247-253.
8. Chang YC, Lin CY, Hsu CM, Lin HC, Chen YH, Lee-Chen GJ, Su MT, Ro LS, Chen CM, Hsieh-Li HM (2011) Neuroprotective effects of granulocyte-colony stimulating factor in a novel transgenic mouse model of SCA17. Journal of neurochemistry 118:288-303.
9. Chen DH, Cimino PJ, Ranum LP, Zoghbi HY, Yabe I, Schut L, Margolis RL, Lipe HP, Feleke A, Matsushita M, Wolff J, Morgan C, Lau D, Fernandez M, Sasaki H, Raskind WH, Bird TD (2005) The clinical and genetic spectrum of spinocerebellar ataxia 14. Neurology 64:1258-1260.
10. Chen T, Fei F, Jiang XF, Zhang L, Qu Y, Huo K, Fei Z (2012) Down-regulation of Homer1b/c attenuates glutamate-mediated excitotoxicity through endoplasmic reticulum and mitochondria pathways in rat cortical neurons. Free radical biology & medicine 52:208-217.
11. Clausen A, McClanahan T, Ji SG, Weiss JH (2013) Mechanisms of rapid reactive oxygen species generation in response to cytosolic $Ca^{2+)}$ or $Zn^{(2+)}$ loads in cortical neurons. PloS one 8:e83347.

12. Cui W, Hu S, Chan HH, Luo J, Li W, Mak S, Choi TC, Rong J, Carlier PR, Han Y (2013) Bis(12)-hupyridone, a novel acetylcholinesterase inhibitor, protects against glutamate-induced neuronal excitotoxicity via activating alpha7 nicotinic acetylcholine receptor/phosphoinositide 3-kinase/Akt cascade. Chemico-biological interactions 203:365-370.
13. Dargusch R, Piasecki D, Tan S, Liu Y, Schubert D (2001) The role of Bax in glutamate-induced nerve cell death. Journal of neurochemistry 76:295-301.
14. Delgado-Rubin de Celix A, Chowen JA, Argente J, Frago LM (2006) Growth hormone releasing peptide-6 acts as a survival factor in glutamate-induced excitotoxicity. Journal of neurochemistry 99:839-849.
15. Di X, Yan J, Zhao Y, Zhang J, Shi Z, Chang Y, Zhao B (2010) L-theanine protects the APP (Swedish mutation) transgenic SH-SY5Y cell against glutamate-induced excitotoxicity via inhibition of the NMDA receptor pathway. Neuroscience 168:778-786.
16. Dick KA, Ikeda Y, Day JW, Ranum LP (2012) Spinocerebellar ataxia type 5. Handbook of clinical neurology 103:451-459.
17. Duchen MR (2012) Mitochondria, calcium-dependent neuronal death and neurodegenerative disease. European journal of physiology 464:111-121.

18. Duenas AM, Goold R, Giunti P (2006) Molecular pathogenesis of spinocerebellar ataxias. Brain. 129:1357-1370.
19. Evert BO, Wullner U, Schulz JB, Weller M, Groscurth P, Trottier Y, Brice A, Klockgether T (1999) High level expression of expanded full-length ataxin-3 in vitro causes cell death and formation of intranuclear inclusions in neuronal cells. Human molecular genetics 8:1169-1176.
20. Friedman MJ, Li S, Li XJ (2009) Activation of gene transcription by heat shock protein 27 may contribute to its neuronal protection. The Journal of biological chemistry 284:27944-27951
21. Friedman MJ, Wang CE, Li XJ, Li S (2008) Polyglutamine expansion reduces the association of TATA-binding protein with DNA and induces DNA binding-independent neurotoxicity. The Journal of biological chemistry 283:8283-8290.
22. Gao M, Zhang WC, Liu QS, Hu JJ, Liu GT, Du GH (2008) Pinocembrin prevents glutamate-induced apoptosis in SH-SY5Y neuronal cells via decrease of bax/bcl-2 ratio. European journal of pharmacology 591:73-79.
23. Ghosh T, Pandey N, Maitra A, Brahmachari SK, Pillai B (2007) A role for voltage-dependent anion channel Vdac1 in polyglutamine-mediated neuronal cell death. PloS one 2:e1170.
24. Gostout B, Liu Q, Sommer SS (1993) "Cryptic" repeating triplets of

purines and pyrimidines (cRRY(i)) are frequent and polymorphic: analysis of coding cRRY(i) in the proopiomelanocortin (POMC) and TATA-binding protein (TBP) genes. American journal of human genetics 52:1182-1190.

25. Henshall, DC. (2007) Apoptosis signaling pathways in seizure-induced neuronal death and epilepsy. Biochem Soc Trans. 35(2):421-423.
26. Hirashima Y, Kurimoto M, Nogami K, Endo S, Saitoh M, Ohtani O, Nagata T, Muraguchi A, Takaku A (1999) Correlation of glutamate-induced apoptosis with caspase activities in cultured rat cerebral cortical neurons. Brain Res 849:109-118.
27. Huang S, Ling JJ, Yang S, Li XJ, Li S (2011) Neuronal expression of TATA box-binding protein containing expanded polyglutamine in knock-in mice reduces chaperone protein response by impairing the function of nuclear factor-Y transcription factor. Brain : a journal of neurology 134:1943-1958.
28. Ishikawa K, Ishiguro T, Takahashi M, Sato N, Amino T, Niimi Y, Mizusawa H (2009) Molecular genetic approach to spinocerebellar ataxias. Clinical neurology 49:907-909.
29. Jang JY, Kim HN, Kim YR, Choi YW, Choi YH, Lee JH, Shin HK, Choi BT. Hexane extract from Polygonum multiflorum attenuates glutamate-induced apoptosis in primary cultured cortical

neurons (2013) J Ethnopharmacol. 145(1):261-268.

30. Kasumu A, Bezprozvanny I (2012) Deranged calcium signaling in Purkinje cells and pathogenesis in spinocerebellar ataxia 2 (SCA2) and other ataxias. Cerebellum 11:630-639.
31. Kim S, Nollen EA, Kitagawa K, Bindokas VP, Morimoto RI (2002) Polyglutamine protein aggregates are dynamic. Nature cell biology 4:826-831.
32. Koeppen AH (2005) The pathogenesis of spinocerebellar ataxia. Cerebellum 4:62-73.
33. Koide R, Kobayashi S, Shimohata T, Ikeuchi T, Maruyama M, Saito M, Yamada M, Takahashi H, Tsuji S (1999) A neurological disease caused by an expanded CAG trinucleotide repeat in the TATA-binding protein gene: a new polyglutamine disease? Human molecular genetics 8:2047-2053.
34. Kristal BS, Dubinsky JM (1997) Mitochondrial permeability transition in the central nervous system: induction by calcium cycling-dependent and -independent pathways. Journal of neurochemistry 69:524-538.
35. Kroemer G, Dallaporta B, Resche-Rigon M (1998) The mitochondrial death/life regulator in apoptosis and necrosis. Annual review of physiology 60:619-642.

36. Lai TW, Zhang S, Wang YT (2013) Excitotoxicity and stroke: Identifying novel targets for neuroprotection. Progress in neurobiology.
37. Lau A, Tymianski M (2010) Glutamate receptors, neurotoxicity and neurodegeneration. Pflugers Archiv : European journal of physiology 460:525-542.Lee, L. C., et al. (2009). "Altered expression of HSPA5, HSPA8 and PARK7 in spinocerebellar ataxia type 17 identified by 2-dimensional fluorescence difference in gel electrophoresis." Clin Chim Acta 400(1-2): 56-62.
38. Li J, O W, Li W, Jiang ZG, Ghanbari HA (2013) Oxidative stress and neurodegenerative disorders. International journal of molecular sciences 14:24438-24475.
39. Lee, L. C., et al. (2009). "Altered expression of HSPA5, HSPA8 and PARK7 in spinocerebellar ataxia type 17 identified by 2-dimensional fluorescence difference in gel electrophoresis." Clin Chim Acta 400(1-2): 56-62.
40. Lin MT, Beal MF (2006) Mitochondrial dysfunction and oxidative stress in neurodegenerative diseases. Nature 443:787-795.
41. Liu X, Zhu XZ (1999) Roles of p53, c-Myc, Bcl-2, Bax and caspases in glutamate-induced neuronal apoptosis and the possible neuroprotective mechanism of basic fibroblast growth factor. Brain research Molecular brain research 71:210-216.

42. Ma S, Liu H, Jiao H, Wang L, Chen L, Liang J, Zhao M, Zhang X (2012) Neuroprotective effect of ginkgolide K on glutamate-induced cytotoxicity in PC 12 cells via inhibition of ROS generation and Ca^{2+} influx. Neurotoxicology 33:59-69.
43. Margolis RL, O'Hearn E, Holmes SE, Srivastava AK, Mukherji M, Sinha KK (1993) Spinocerebellar Ataxia Type 12. Gene Reviews
44. Matilla-Duenas A, Sanchez I, Corral-Juan M, Davalos A, Alvarez R, Latorre P (2010) Cellular and molecular pathways triggering neurodegeneration in the spinocerebellar ataxias. Cerebellum 9:148-166.
45. Matsuura T, Yamagata T, Burgess DL, Rasmussen A, Grewal RP, Watase K, Khajavi M, McCall AE, Davis CF, Zu L, Achari M, Pulst SM, Alonso E, Noebels JL, Nelson DL, Zoghbi HY, Ashizawa T (2000) Large expansion of the ATTCT pentanucleotide repeat in spinocerebellar ataxia type 10. Nature genetics 26:191-194.
46. Mattson MP (2008) Glutamate and neurotrophic factors in neuronal plasticity and disease. Annals of the New York Academy of Sciences 1144:97-112.
47. McStay GP, Clarke SJ, Halestrap AP (2002) Role of critical thiol groups on the matrix surface of the adenine nucleotide translocase in the mechanism of the mitochondrial permeability transition pore. The Biochemical journal 367:541-548.

48. Miao Y, Dong LD, Chen J, Hu XC, Yang XL, Wang Z (2012) Involvement of calpain/p35-p25/Cdk5/NMDAR signaling pathway in glutamate-induced neurotoxicity in cultured rat retinal neurons. PloS one 7:e42318.
49. Misceo D, Fannemel M, Baroy T, Roberto R, Tvedt B, Jaeger T, Bryn V, Stromme P, Frengen E (2009) SCA27 caused by a chromosome translocation: further delineation of the phenotype. Neurogenetics 10:371-374.
50. Mutsuddi M, Rebay I (2005) Molecular genetics of spinocerebellar ataxia type 8 (SCA8). RNA biology 2:49-52.
51. Nakamura K, Jeong SY, Uchihara T, Anno M, Nagashima K, Nagashima T, Ikeda S, Tsuji S, Kanazawa I (2001) SCA17, a novel autosomal dominant cerebellar ataxia caused by an expanded polyglutamine in TATA-binding protein. Human molecular genetics 10:1441-1448.
52. Orr HT (2012) Cell biology of spinocerebellar ataxia. The Journal of cell biology 197:167-177.
53. Orr HT, Zoghbi HY (2007) Trinucleotide repeat disorders. Annual review of neuroscience 30:575-621.
54. Paulson H (2009) The spinocerebellar ataxias. J Neuroophthalmol 29(3):227-237.
55. Pfeiffer A, Jaeckel M, Lewerenz J, Noack R, Pouya A, Schacht T,

Hoffmann C, Winter J, Schweiger S, Schafer MK, Methner A (2013) Mitochondrial function and energy metabolism in neuronal HT22 cells resistant to oxidative stress. British journal of pharmacology.

56. Pivovarova NB, Stanika RI, Kazanina G, Villanueva I, Andrews SB (2013) The interactive roles of zinc and calcium in mitochondrial dysfunction and neurodegeneration. Journal of neurochemistry.
57. Popiel HA, Nagai Y, Onodera O, Inui T, Fujikake N, Urade Y, Strittmatter WJ, Burke JR, Ichikawa A, Toda T (2004) Disruption of the toxic conformation of the expanded polyglutamine stretch leads to suppression of aggregate formation and cytotoxicity. Biochemical and biophysical research communications 317:1200-1206.
58. Proctor CJ, Tangeman PJ, Ardley HC (2010) Modelling the role of UCH-L1 on protein aggregation in age-related neurodegeneration. PloS one 5:e13175.
59. Rana S. Moubarak VJY, Cédric Artus, Aïda Bouharrour, Peter A. Greer, Josiane Menissier-de Murcia and Santos A. Susin, (2007) Sequential Activation of Poly(ADP-Ribose) Polymerase 1, Calpains, and Bax Is Essential in Apoptosis-Inducing Factor-Mediated Programmed Necrosis. Mol Cell Biol 27:4844-4862
60. Reid SJ, Rees MI, van Roon-Mom WM, Jones AL, MacDonald ME, Sutherland G, During MJ, Faull RL, Owen MJ, Dragunow M, Snell RG (2003) Molecular investigation of TBP allele length: a SCA17

cellular model and population study. Neurobiology of disease 13:37-45.

61. Rolfs A, Koeppen AH, Bauer I, Bauer P, Buhlmann S, Topka H, Schols L, Riess O (2003) Clinical features and neuropathology of autosomal dominant spinocerebellar ataxia (SCA17). Annals of neurology 54:367-375.
62. Roshan R, Ghosh T, Gadgil M, Pillai B (2012) Regulation of BACE1 by miR-29a/b in a cellular model of Spinocerebellar Ataxia 17. RNA biology 9:891-899.
63. Sakahira H, Breuer P, Hayer-Hartl MK, Hartl FU (2002) Molecular chaperones as modulators of polyglutamine protein aggregation and toxicity. Proceedings of the National Academy of Sciences of the United States of America 99:16412-16418.
64. Seidel K, Siswanto S, Brunt ER, den Dunnen W, Korf HW, Rub U (2012) Brain pathology of spinocerebellar ataxias. Acta neuropathologica 124:1-21.
65. Silveira I, Miranda C, Guimaraes L, Moreira MC, Alonso I, Mendonca P, Ferro A, Pinto-Basto J, Coelho J, Ferreirinha F, Poirier J, Parreira E, Vale J, Januario C, Barbot C, Tuna A, Barros J, Koide R, Tsuji S, Holmes SE, Margolis RL, Jardim L, Pandolfo M, Coutinho P, Sequeiros J (2002) Trinucleotide repeats in 202 families with ataxia: a small expanded (CAG)n allele at the SCA17 locus.

Archives of neurology 59:623-629.

66. Sun ZW, Zhang L, Zhu SJ, Chen WC, Mei B (2010) Excitotoxicity effects of glutamate on human neuroblastoma SH-SY5Y cells via oxidative damage. Neuroscience bulletin 26:8-16.
67. Tan, J. W., et al. (2013). "Neuroprotective effects of biochanin A against glutamate-induced cytotoxicity in PC12 cells via apoptosis inhibition." Neurochem Res 38(3): 512-518.
68. Uchihara T, Fujigasaki H, Koyano S, Nakamura A, Yagishita S, Iwabuchi K (2001) Non-expanded polyglutamine proteins in intranuclear inclusions of hereditary ataxias--triple-labeling immunofluorescence study. Acta neuropathologica 102:149-152.
69. Votyakova TV, Reynolds IJ (2005) Ca^{2+}-induced permeabilization promotes free radical release from rat brain mitochondria with partially inhibited complex I. Journal of neurochemistry 93:526-537.
70. Xu MF, Xiong YY, Liu JK, Qian JJ, Zhu L, Gao J (2012) Asiatic acid, a pentacyclic triterpene in Centella asiatica, attenuates glutamate-induced cognitive deficits in mice and apoptosis in SH-SY5Y cells. Acta pharmacologica Sinica 33:578-587.
71. Yang JL, Sykora P, Wilson DM, 3rd, Mattson MP, Bohr VA (2011) The excitatory neurotransmitter glutamate stimulates DNA repair to increase neuronal resiliency. Mechanisms of ageing and development 132:405-411.

72. Zhang C, Du F, Shi M, Ye R, Cheng H, Han J, Ma L, Cao R, Rao Z, Zhao G (2012) Ginsenoside Rd protects neurons against glutamate-induced excitotoxicity by inhibiting Ca^{2+} influx. Cellular and molecular neurobiology 32:121-128.
73. Zhang C, Yuan XR, Li HY, Zhao ZJ, Liao YW, Wang XY, Su J, Sang SS, Liu Q (2014) Downregualtion of dynamin-related protein 1 attenuates glutamate-induced excitotoxicity via regulating mitochondrial function in a calcium dependent manner in HT22 cells. Biochemical and biophysical research communications 443:138-143.
74. Zhang K, Li YJ, Yang Q, Gerile O, Yang L, Li XB, Guo YY, Zhang N, Feng B, Liu SB, Zhao MG (2013) Neuroprotective effects of oxymatrine against excitotoxicity partially through down-regulation of NR2B-containing NMDA receptors. Phytomedicine : international journal of phytotherapy and phytopharmacology 20:343-350.
75. Zhang, Y. and B. R. Bhavnani (2006) Glutamate-induced apoptosis in neuronal cells is mediated via caspase-dependent and independent mechanisms involving calpain and caspase-3 proteases as well as apoptosis inducing factor (AIF) and this process is inhibited by equine estrogens. BMC Neurosci 7: 49.

7 Figures

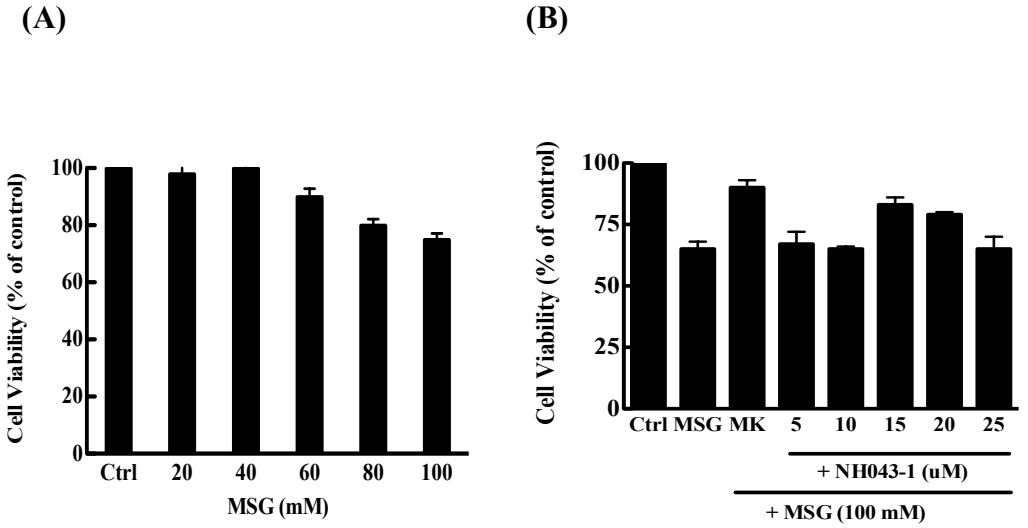

Figure 1. NH043-1 improved MSG-induced cell death by using MTT assay in SH-SY5Y cells.

(A) Cell death was measured after treating MSG with various concentrations in 2 x 10^4 SH-SY5Y cells. (B) Cell viabilities were measured after treating with 100 mM MSG for 24 h in the absence or presence of NH043-1 at indicated doses, or NMDA receptor antagonist, MK801, in SH-SY5Y cells. Data were the mean values of three independent experiments.

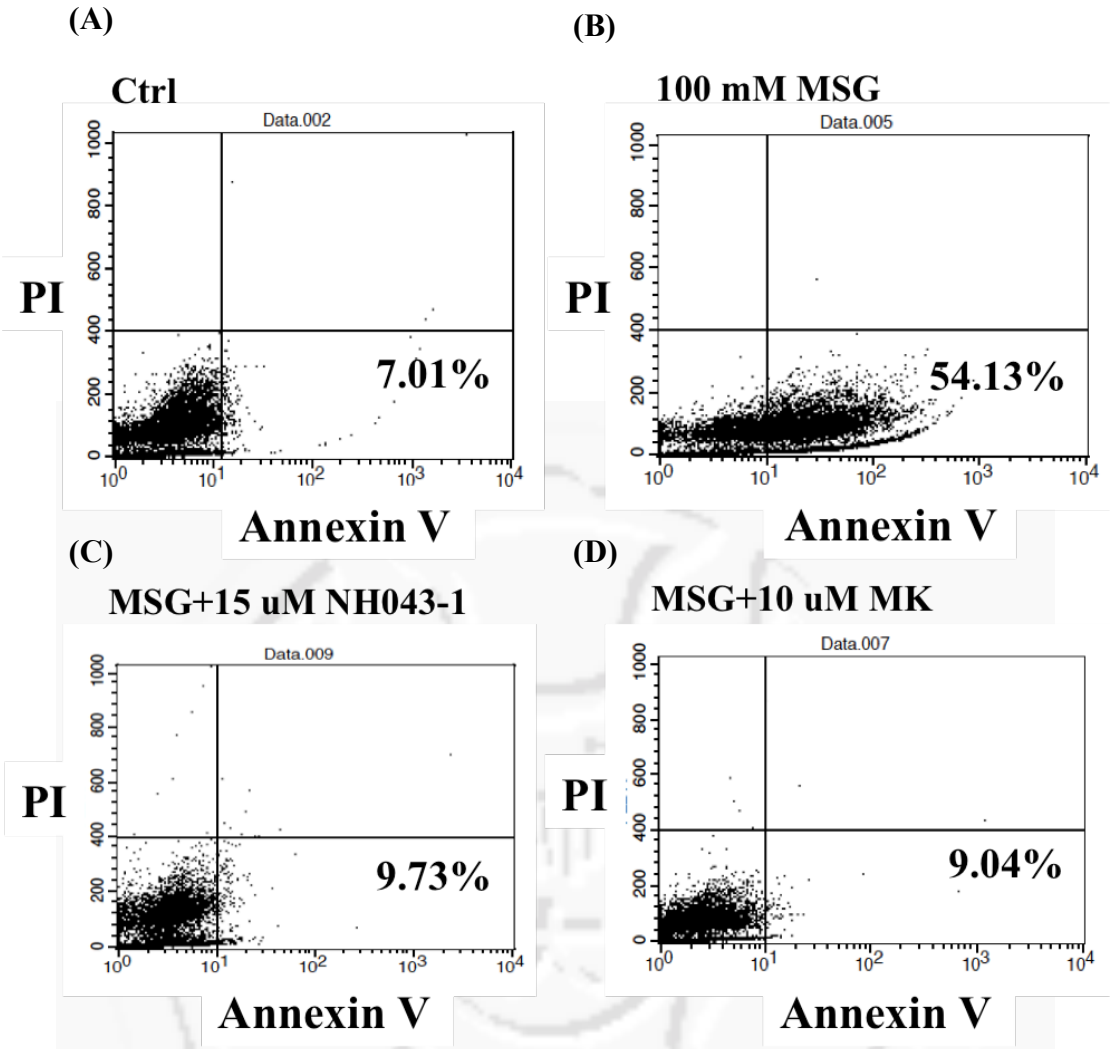

Figure 2. NH043-1 inhibited MSG-induced cell apoptosis by Annexin-V staining.

Apoptosis detection was measured after treating with 100 mM MSG and 15 uM NH043-1 or 10 uM MK801 for 24 h in 1 x 10^6 SH-SY5Y cells. Cells were stained with Annexin-V/PI and measured with a flow cytometry. (A) Control (B) 100 mM MSG (C) 100 mM MSG with 15 uM NH043-1 or (D) 10 uM MK801.

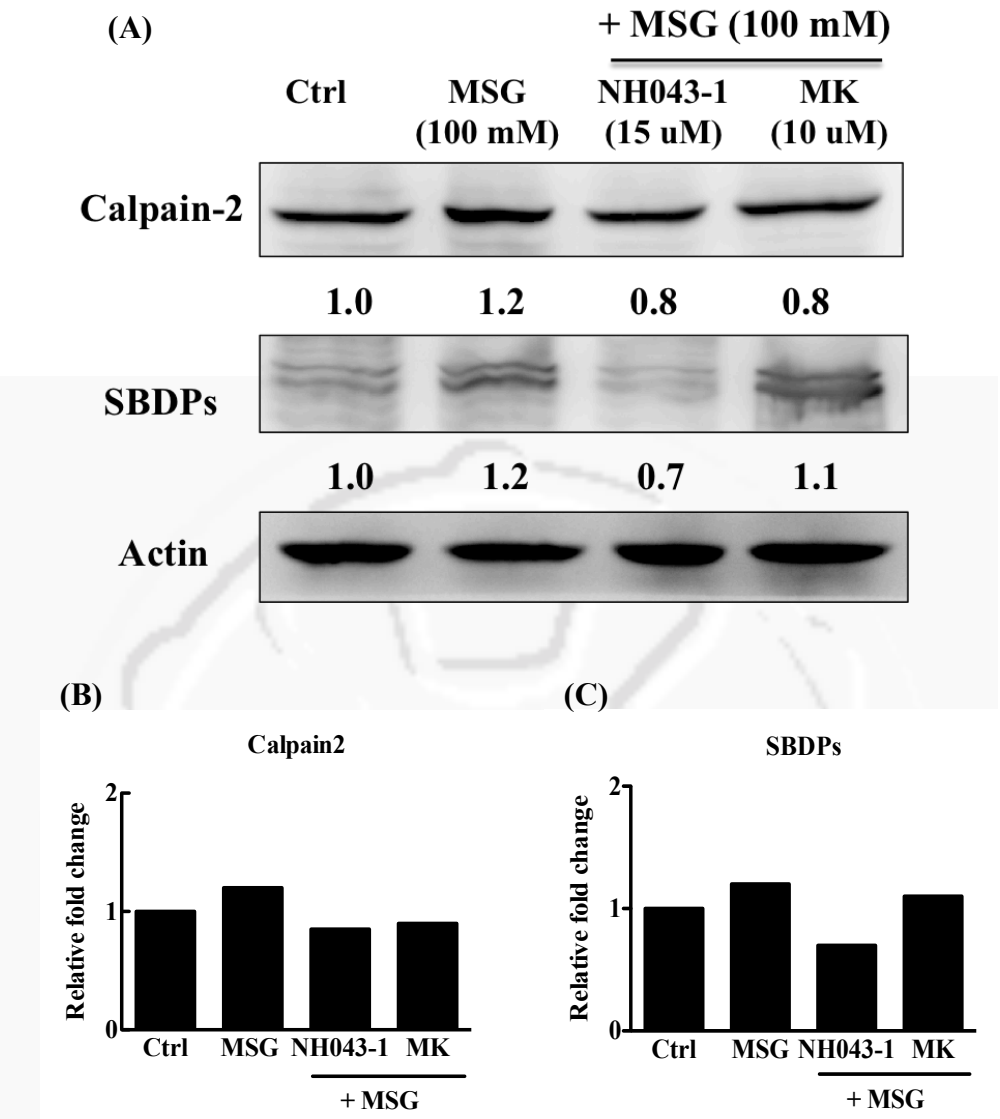

Figure 3. NH043-1 decreased Calpain-2 and SBDPs expressions by MSG in SH-SY5Y cells.

(A) Calpain-2 and SBDPs expressions were measured by western blot analysis after treating with 100 mM MSG and 15 uM NH043-1 or 10 uM MK801 for 6 h in 1 x 10^6 SH-SY5Y cells. (B) and (C) Quantification of the intensities of Calpain-2 and SBDPs protein bands was analyzed by ImageJ software and actin was used as loading control.

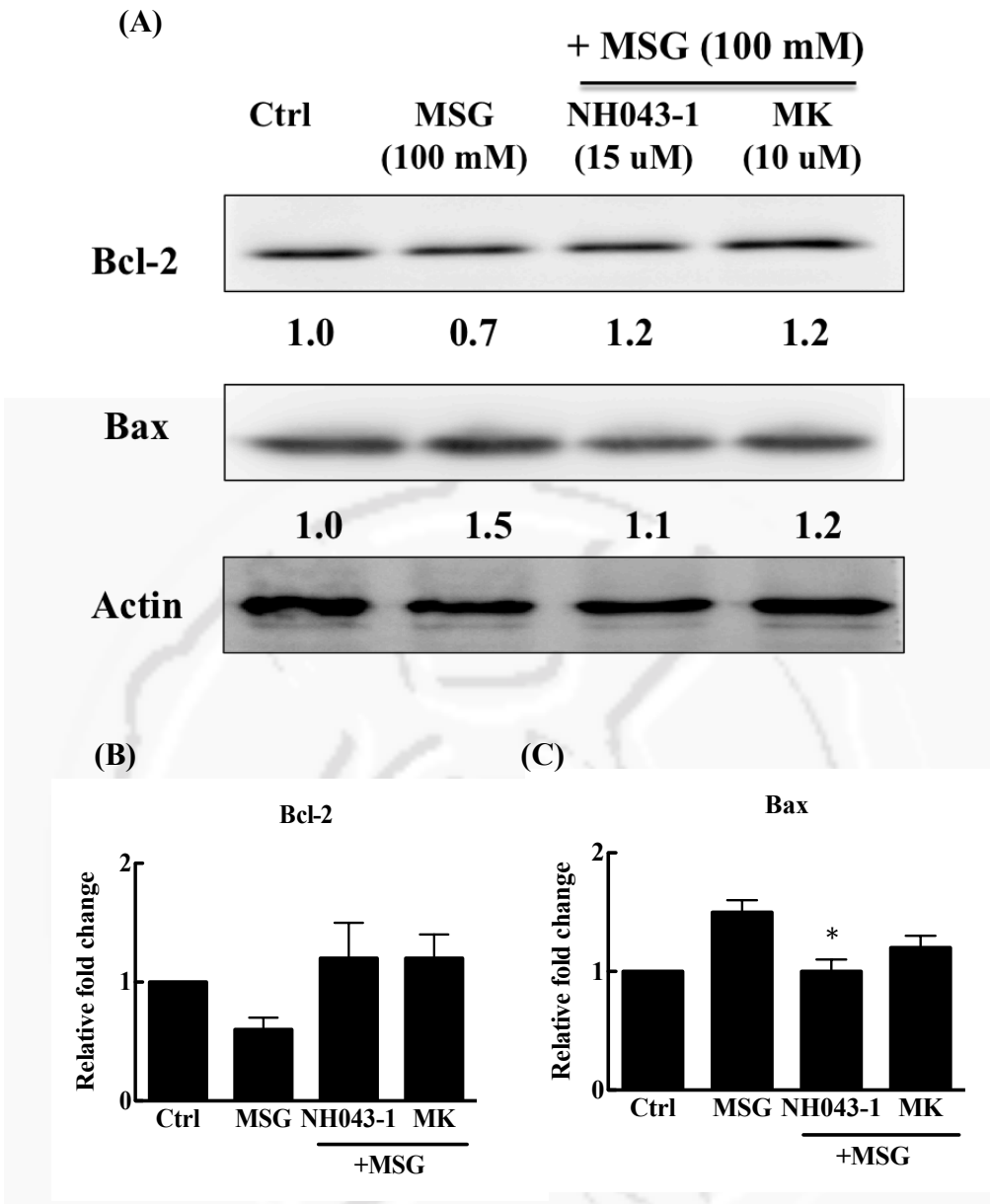

Figure 4. Effects of NH043-1 on the changes of Bcl-2 and Bax expressions by MSG in SH-SY5Y cells

(A) Bcl-2 and Bax expressions were measured by western blot analysis after treating with 100 mM MSG and 15 uM NH043-1 or 10 uM MK801 for 6 hours in 1 x 10^6 SH-SY5Y cells. (B) and (C) Quantification of the intensities of Bcl-2 and Bax protein bands was detected by ImageJ software and actin was used as loading control. The results were shown as mean ± SEM, n=3, $*p < 0.05$, comparing to MSG group.

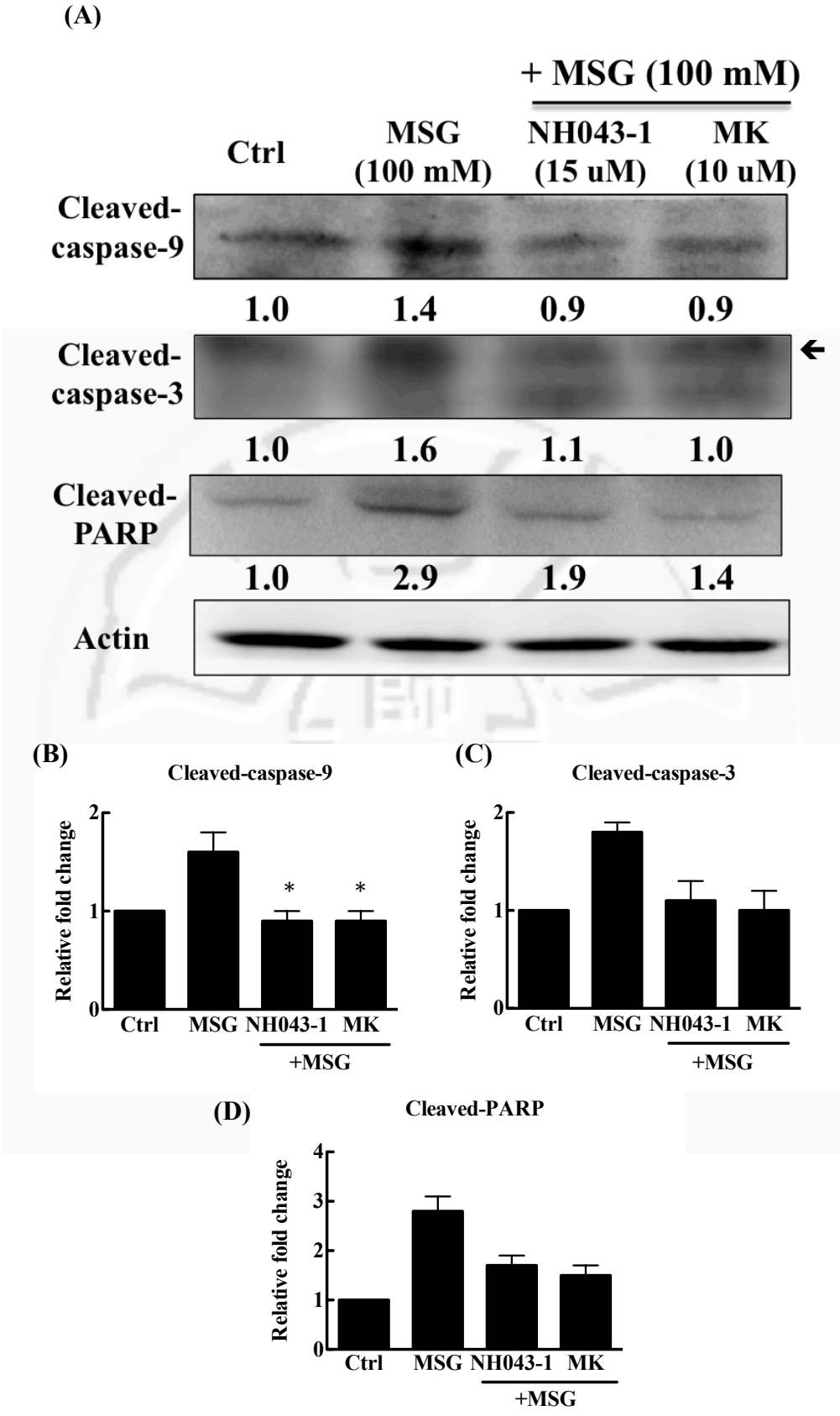
(A)
+ MSG (100 mM)
Ctrl
MSG (100 mM)
NH043-1 (15 uM)
MK (10 uM)
Cleaved-caspase-9
1.0 1.4 0.9 0.9
Cleaved-caspase-3
1.0 1.6 1.1 1.0
Cleaved-PARP
1.0 2.9 1.9 1.4
Actin
(B)
Cleaved-caspase-9
Relative fold change
Ctrl MSG NH043-1 MK
+MSG
(C)
Cleaved-caspase-3
Relative fold change
Ctrl MSG NH043-1 MK
+MSG
(D)
Cleaved-PARP
Relative fold change
Ctrl MSG NH043-1 MK
+MSG

Figure 5. Effects of NH043-1 on cleaved-caspase-9, cleaved-caspase-3, and cleaved-PARP expressions by MSG induction in SH-SY5Y cells

(A) 1 x 10^6 SH-SY5Y cells were treated with 100 mM and 15 uM NH043-1 or 10 uM MK801 for 24 h. The expressions of cleaved-caspase-9, cleaved-caspase-3, and cleaved-PARP were measured by Western blot analysis. (B), (C), and (D) Quantification of the intensities of cleaved-caspase-9, cleaved-caspase-3, and cleaved-PARP protein bands was detected by ImageJ software and actin was used as loading control. The results were shown as mean ± SEM, n=3, $*p < 0.05$, comparing to MSG group.

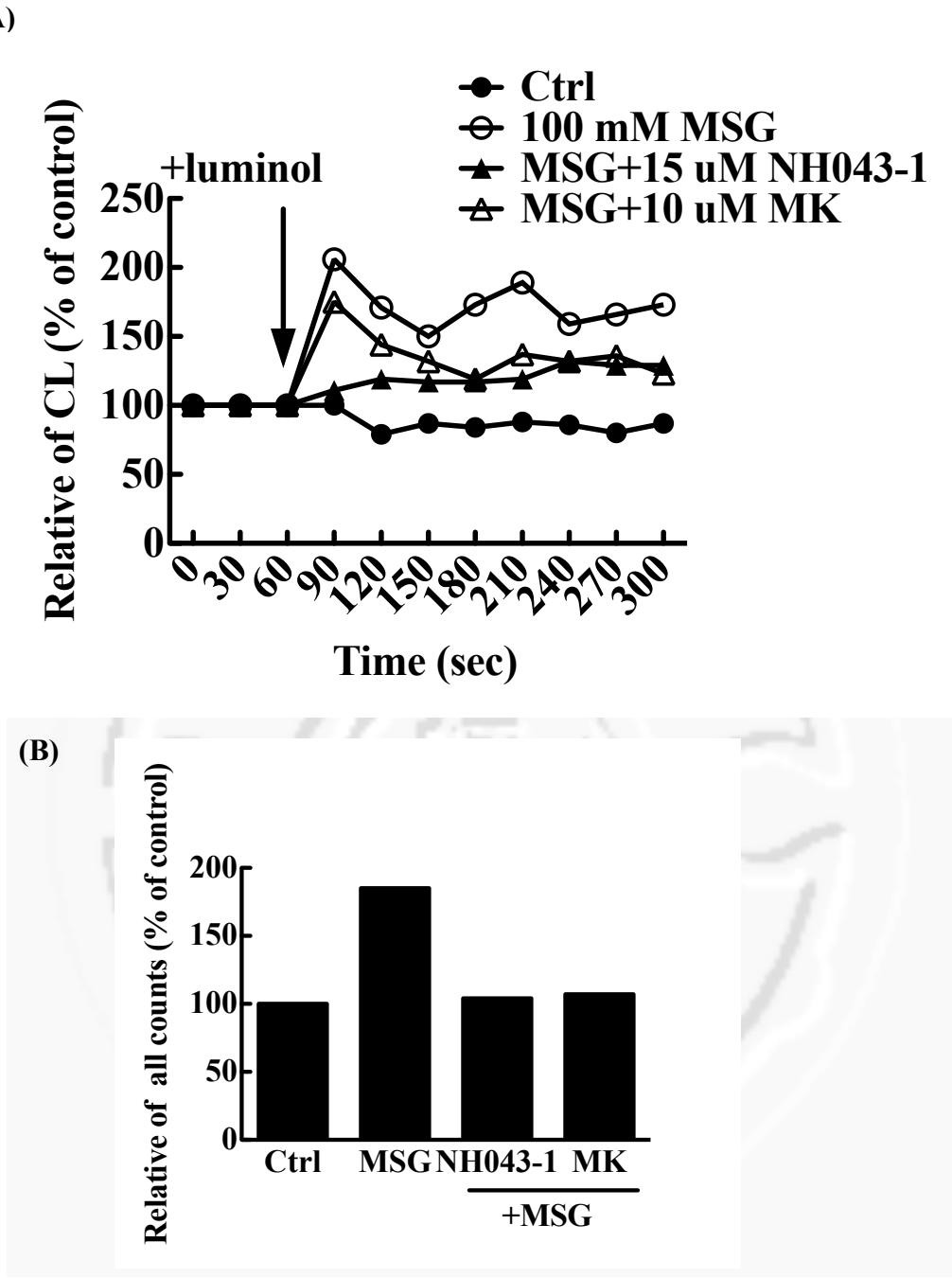

Figure 6. NH043-1 decreased the ROS production in SH-SY5Y cells by MSG.

(A) ROS productions were measured by CL analysis after treating with 100 mM MSG for 24 h in the absence or presence of 15 uM NH043-1 or NMDA receptor antagonist, 10 uM MK801, in 1 x 10^6 SH-SY5Y cells with a luminol-enhanced chemiluminescence detector. (B) Total counts of ROS production.

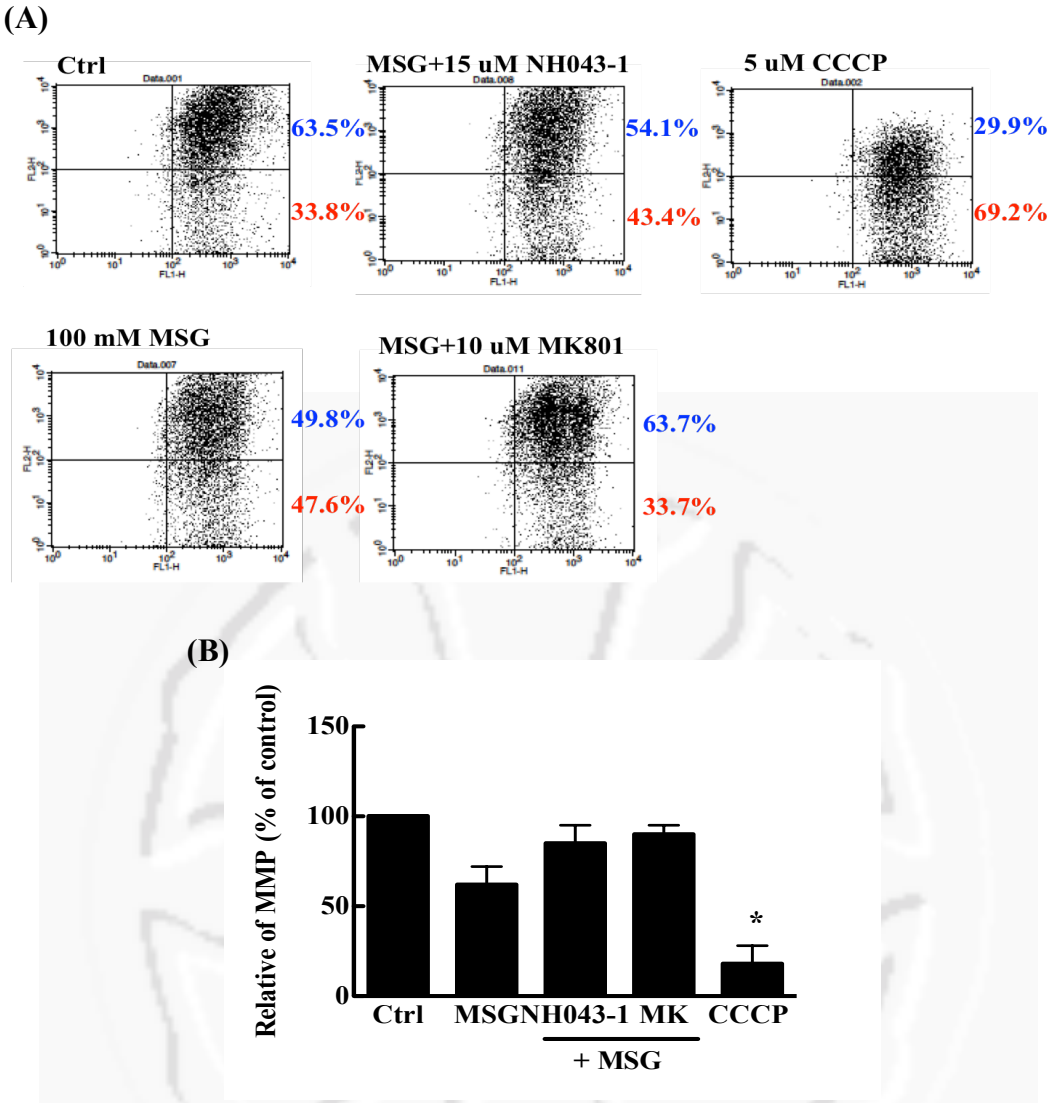

Figure 7. NH043-1 rescued MSG-induced loss of MMP by using JC-1 staining in SH-SY5Y cells.

(A) Loss of MMP were measured after treating with 100 mM MSG for 12 hours in the absence or presence of 15 uM NH043-1 or NMDA receptor antagonist, 10 uM MK801 in 1 x 10^6 SH-SY5Y cells, with JC-1 staining and analyzed with a flow cytometry. The treatments included control, 100 mM MSG, 100 mM MSG with 15 uM NH043-1, 100 mM MSG with 10 uM MK801, and 5 uM CCCP (disruptor of electron transport chain). (B) The ratio of JC-1 oligomer/monomer was determined. The results were shown as mean ± SEM, n=3, *$p < 0.05$, comparing to MSG group.

(A)

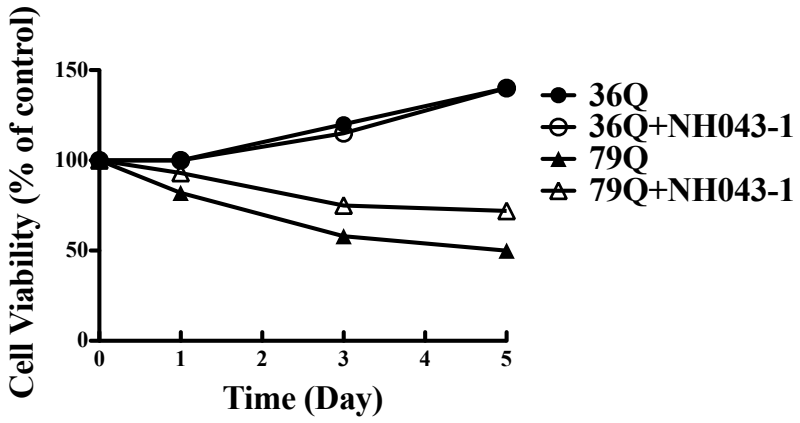
Cell Viability (% of control)
150
100
50
0
0
1
2
3
4
5
Time (Day)
36Q
36Q+NH043-1
79Q
79Q+NH043-1

(B)

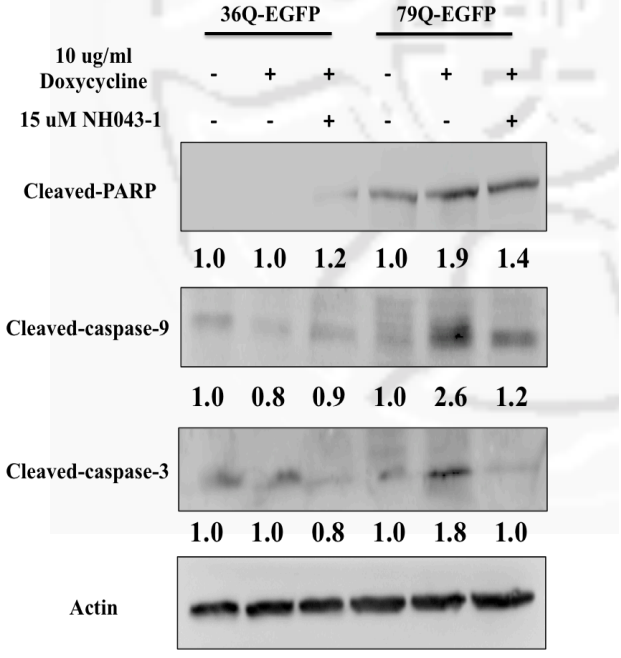
36Q-EGFP
79Q-EGFP
10 ug/ml Doxycycline
- + + - + +
15 uM NH043-1
- - + - - +
Cleaved-PARP
1.0 1.0 1.2 1.0 1.9 1.4
Cleaved-caspase-9
1.0 0.8 0.9 1.0 2.6 1.2
Cleaved-caspase-3
1.0 1.0 0.8 1.0 1.8 1.0
Actin

(C)

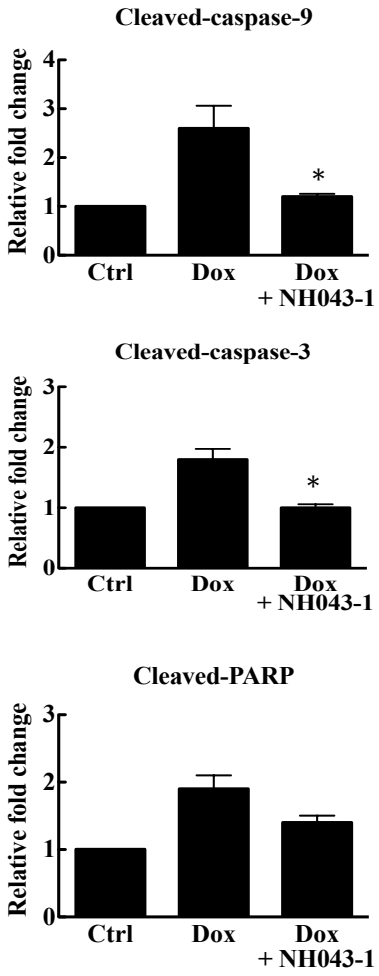
Cleaved-caspase-9
Relative fold change
Ctrl
Dox
Dox + NH043-1
Cleaved-caspase-3
Relative fold change
Ctrl
Dox
Dox + NH043-1
Cleaved-PARP
Relative fold change
Ctrl
Dox
Dox + NH043-1

Figure 8. NH043-1 improved cell viability and inhibited cleaved-caspase-9, cleaved-caspase-3, and cleaved-PARP expressions after doxycycline induction in nTBP/Q_{79} cells.

(A) 1.0 x 10^6 nTBP/Q_{36} and nTBP/Q_{79} cells were induced with 10 ug/mL doxycycline for 1, 3, and 5 d after pretreatment of 15 uM NH043-1 for 1 h. Cell viabilities were measured using MTT assay. (B) 1.0 x 10^6 nTBP/Q_{36} and nTBP/Q_{79} cells were induced with 10 ug/mL doxycycline for 5 d after pretreatment of 15 uM NH043-1 for 1 h. The expressions of cleaved-caspase-9, cleaved-caspase-3, and cleaved-PARP were detected by western blot. (C) Quantitative analysis of the intensities of cleaved-caspase-3, cleaved-caspase-9, and cleaved-PARP protein executed in nTBP/Q_{79} cells by ImageJ software and actin was used as loading control. The results were shown as mean ± SD, n=3, $*p < 0.05$, comparing to Dox group.

(A)

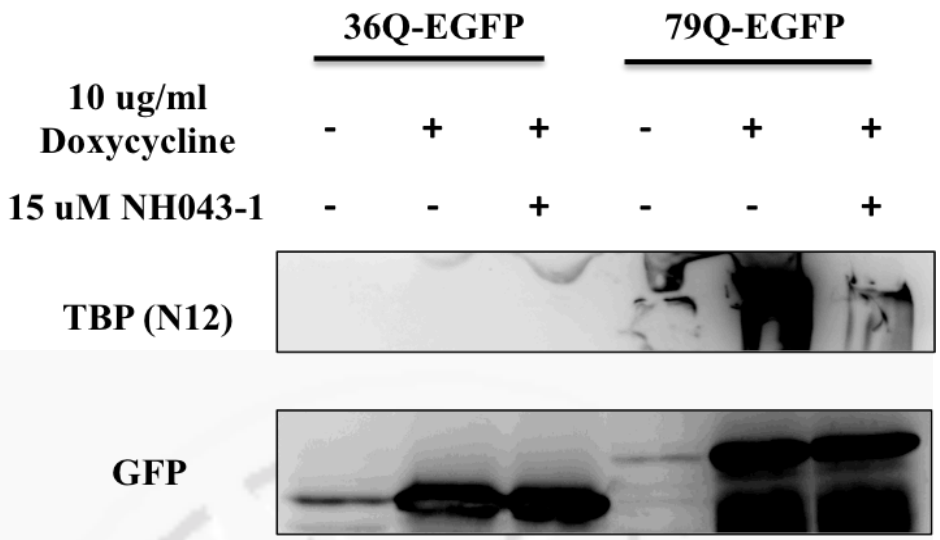
36Q-EGFP
79Q-EGFP
10 ug/ml Doxycycline
- + + - + +
15 uM NH043-1
- - + - - +
TBP (N12)
GFP

(B)

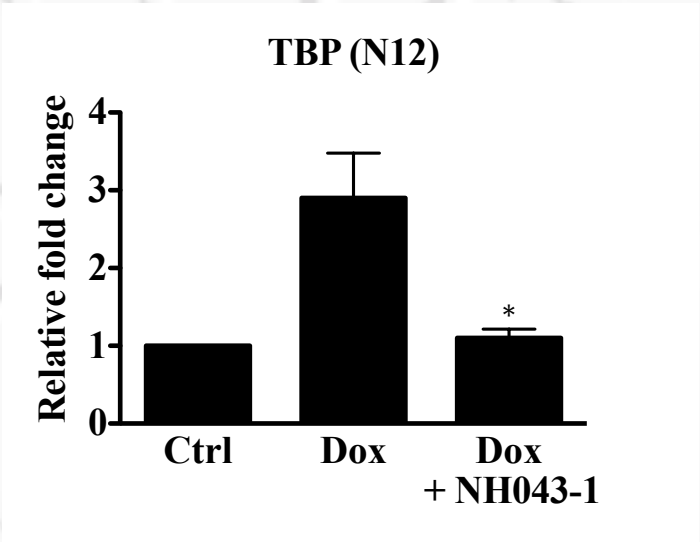
TBP (N12)
Relative fold change
0
1
2
3
4
*
Ctrl
Dox
Dox
+ NH043-1

(C)

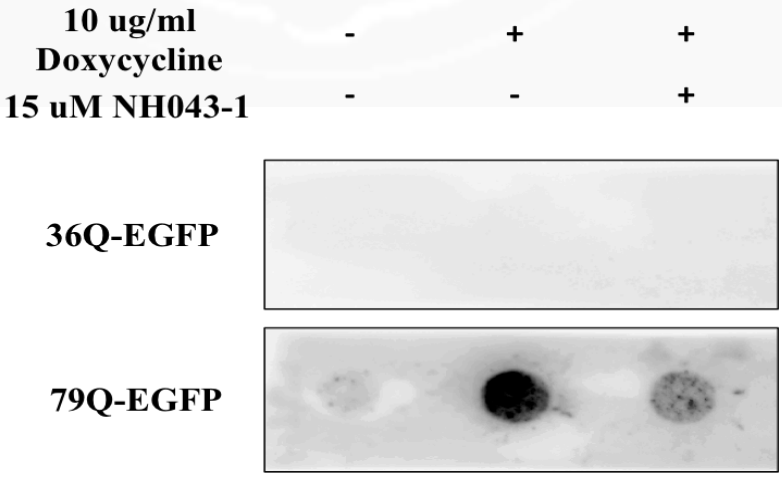
10 ug/ml Doxycycline
- + +
15 uM NH043-1
- - +
36Q-EGFP
79Q-EGFP

Figure 9. Effects of NH043-1 on protein aggregation after doxycycline induction of nTBP/Q_{36} and nTBP/Q_{79} by using dot-blot assay

1.0 x 10^6 nTBP/Q_{36} or nTBP/Q_{79} cells were treated with 10 ug/mL doxycycline for 5 days after pretreatment of 15 uM NH043-1 for 1 hour. Cell lysates were analyzed using anti-TBP (N12) antibody on (A) western blot and (C) dot-blot assay. (B) Quantitative analysis of the intensities of TBP (N12) protein executed in nTBP/Q_{79} cells by ImageJ software. The values represent means ± SD, n=3. *p< 0.05, comparing to Dox group.

(A)

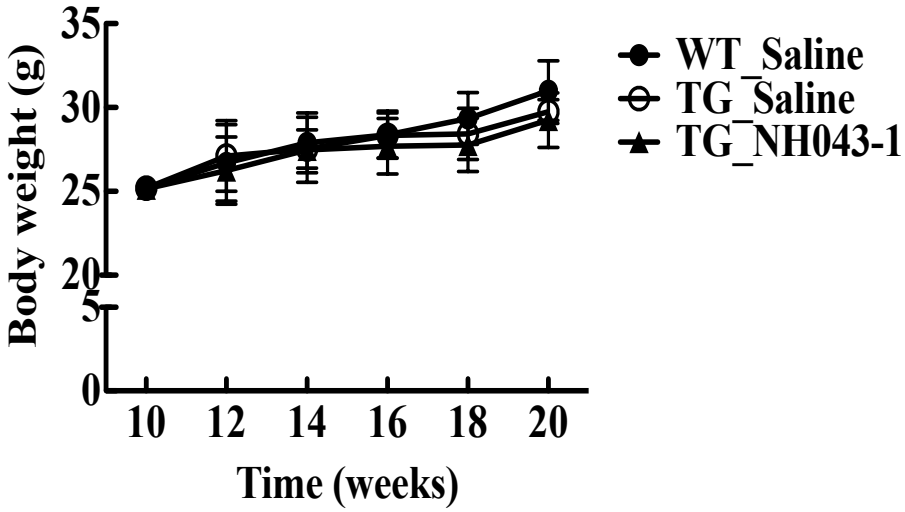

(B)

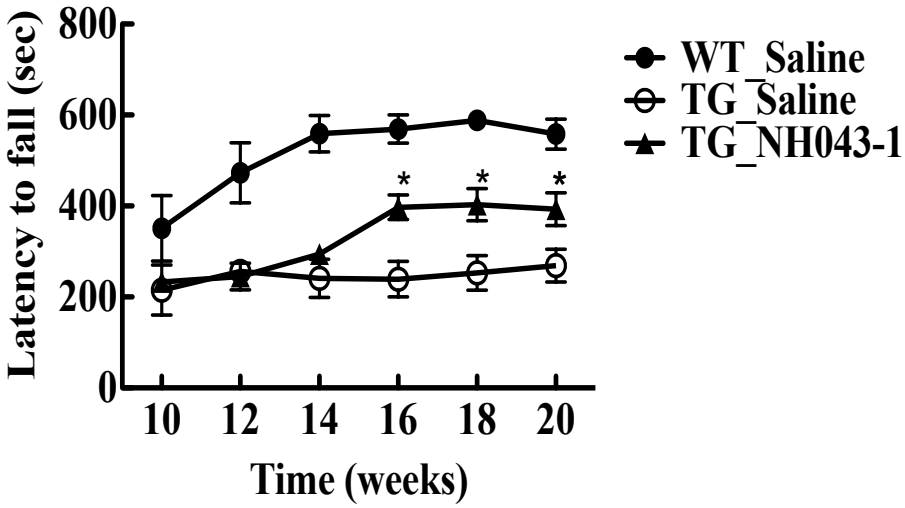

Figure 10. Effects of NH043-1 on body weight and motor performance in SCA17 transgenic mice

Mice were grouped into WT_Saline, TG_Saline, and TG_NH043-1 groups. (A) Mice body weight was measured from 8- to 20-week-old. (B) The performance of motor coordination was determined by rotarod assay. The values represent means ± SD, n=6. *p< 0.05, comparing to TG_Saline group. Mice were intraperitoneal-injected with saline or NH043-1 (4.5 mg/kg) at 10-week by three times a week.

(A)

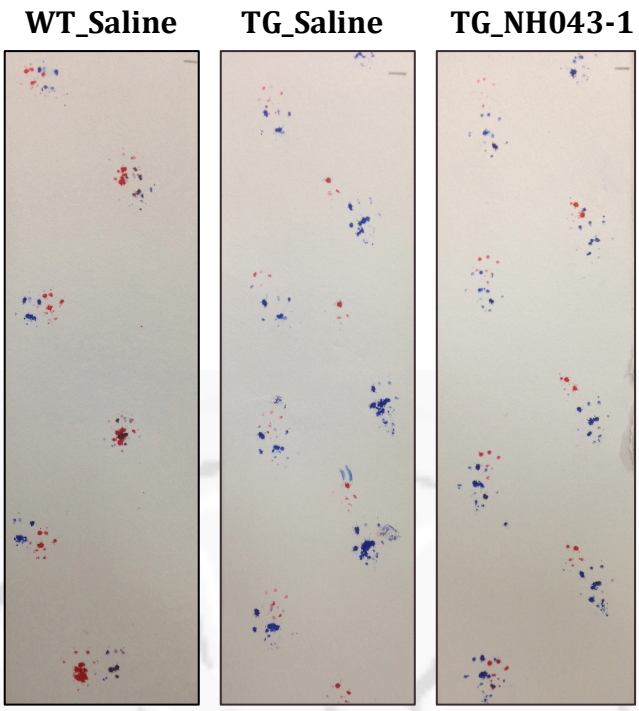
WT_Saline
TG_Saline
TG_NH043-1

(B)

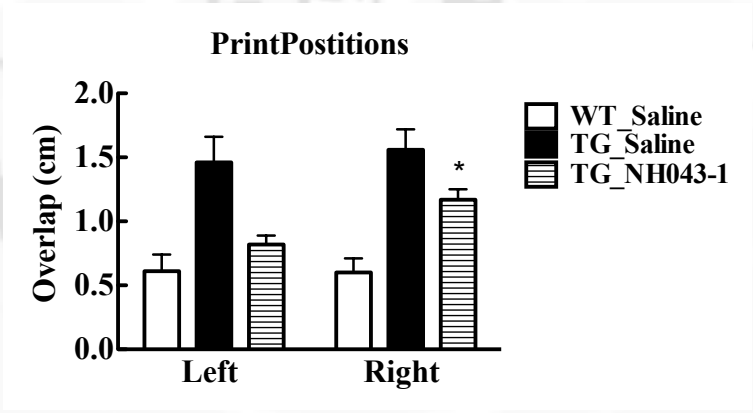
PrintPostitions
Overlap (cm)
2.0
1.5
1.0
0.5
0.0
*
Left
Right
WT_Saline
TG_Saline
TG_NH043-1

(C)

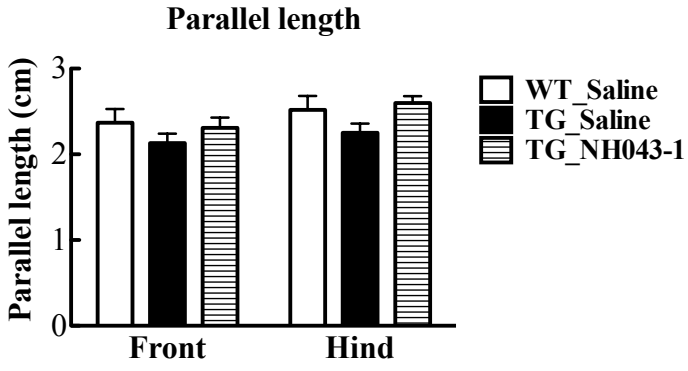
Parallel length
Parallel length (cm)
3
2
1
0
Front
Hind
WT_Saline
TG_Saline
TG_NH043-1

(D)

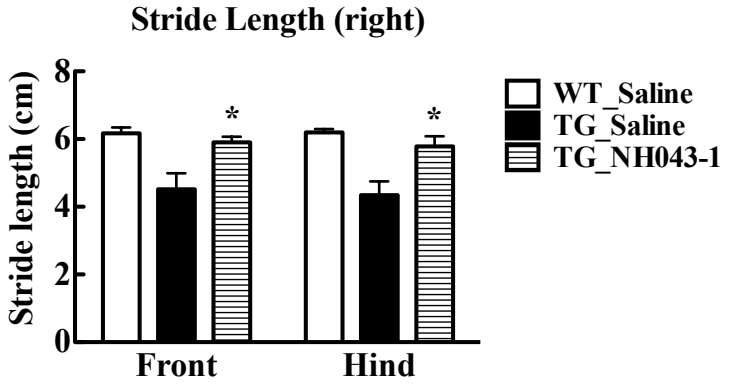

(E)

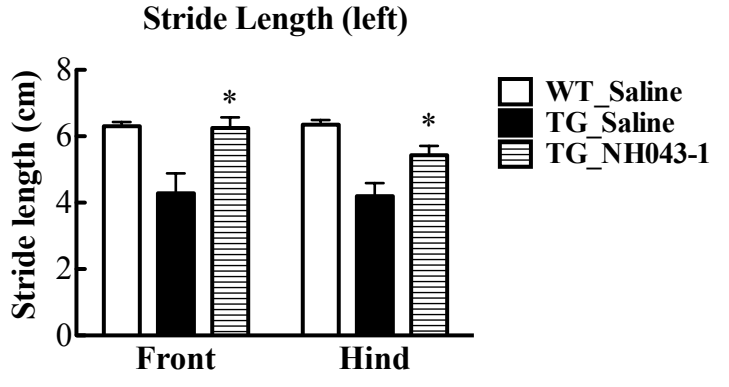

Figure 11. NH043-1 treatment improved gait abnormalities in SAC17 mice.

Footprint analysis of WT_Saline, TG_Saline, and TG_NH043-1 (4.5 mg/kg) mice were performed at 20-week. Mice were intraperitoneal-injected with saline or NH043-1 from 10-week by three times a week. (A) The footprint patterns of WT_Saline, TG_Saline, and TG_NH043-1 were shown. (B) The front/hind footprint overlaps (cm), (C) the parallel length (cm), and (D and E) the front/hind stride lengths (cm). The results were shown as mean ± SEM, n=6, *$p < 0.05$, comparing to TG_Saline group.

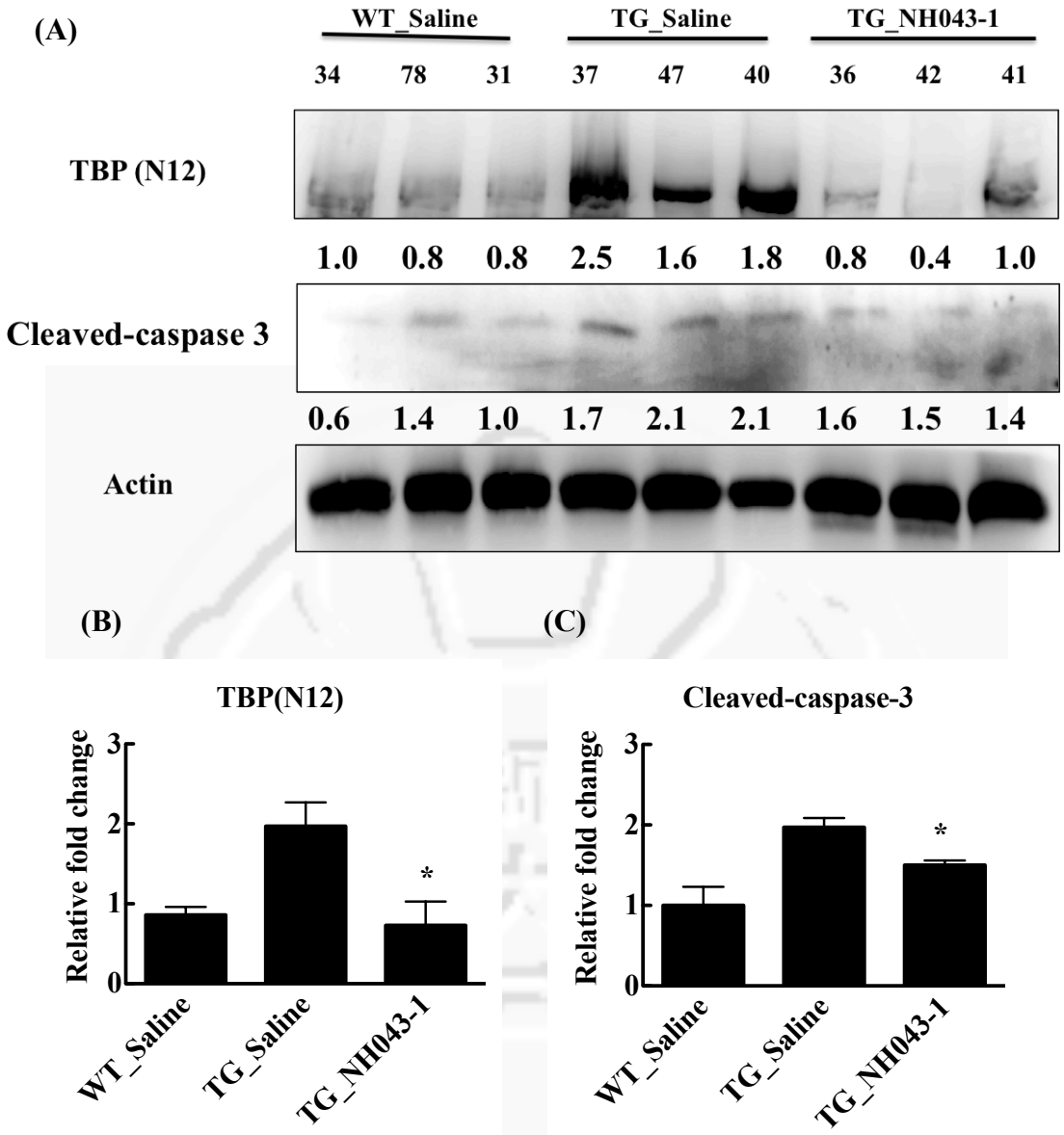

Figure 12. NH043-1 inhibited TBP aggregation and cleaved-caspase-3 expression in SCA17 transgenic mice.

(A) The extent of TBP aggregation [detected using TBP (N12) antibody], and the expression of cleaved-caspase-3 in the cerebella of mice were measured by western blotting at 20-week. (B) and (C) Quantitative analysis of the intensities of TBP (N12) and cleaved-caspase-3 protein executed by ImageJ and actin was used as loading control. The results were shown as mean ± SEM, n=6, *$p < 0.05$, comparing to TG_Saline group.

8 Table

Table 1. IC_{50}-cytotoxicity of nine compounds studied

Compound number	$IC_{50\text{-Cytotoxicity}}$	Compound number	$IC_{50\text{-Cytotoxicity}}$
NH035-1	255 uM	NH046-1	150 uM
NH035-2	60 mM	NH047-1	635 uM
NH043-1	30 uM	NH048-1	800 uM
NH044-1	4 uM	NH049-1	125 uM
NH045-1	210 uM		

9 Supplementary figure

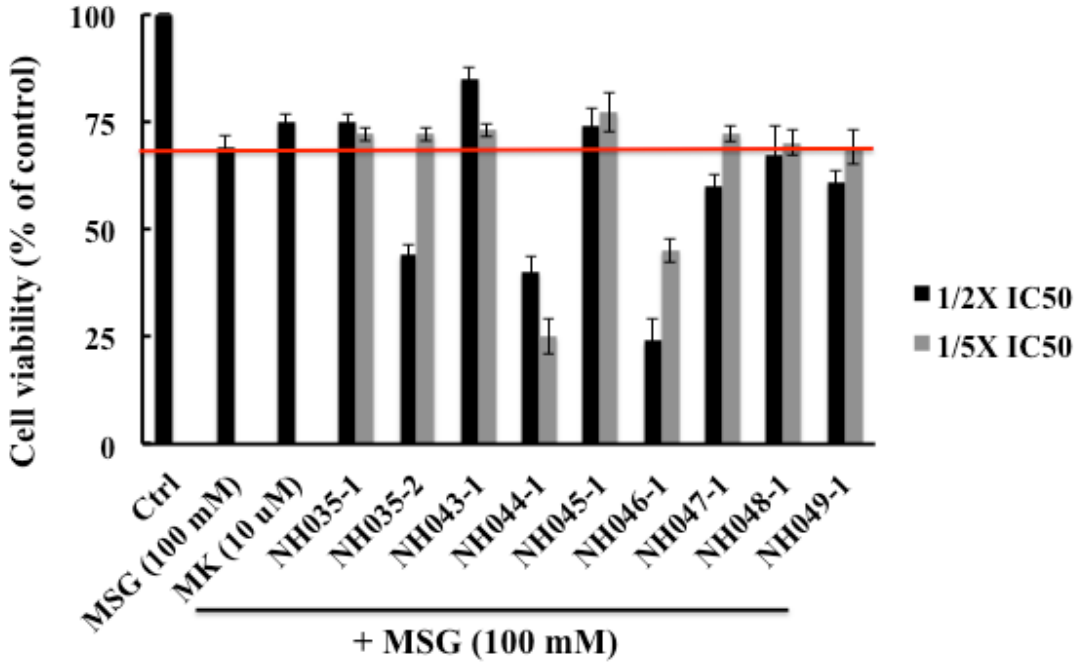

Supplementary figure 1. Effects of nine compounds on MSG-induced cell death in SH-SY5Y cells

2.0 x 10^4 SH-SY5Y cells were pretreated with 1/2x or 1/5x IC_{50} of nine compounds as listed in Table, or 10 uM MK801 for 1 h, then treated with MSG. Cell viability was measured by MTT assay at 24 h treatment.